Dissertation

Comparison of two digitally planned insertion guides for orthodontic mini-implants compared to conventional miniscrew insertion

submitted by

Lea Katharina STURSA

for the Academic Degree of

Doctor of Medical Science (Dr. scient. Med.)

at the

Medical University of Graz

Department of Dental Medicine and Oral Health
Division of Oral Surgery and Orthodontics

under the Supervision of

Univ.- Prof. Univ. FÄ Priv.- Doz. Dr. Brigitte WENDL

2024

Declaration

I hereby confirm that the present diploma thesis is the result of my own independent scholarly work. I also confirm that in all cases, where material from the work of others (in books, articles, essays, dissertations, and on the internet) is acknowledged, quotations and paraphrases are clearly indicated. No material other than that cited in the reference list has been used. I have read and understood the Medical University's regulations and procedures concerning plagiarism.

Furthermore, I hereby declare that if artificial intelligence (AI) tools were used for the generation and/or correction of certain text passages in the creation of this work, such employment was conducted in compliance with ethical principles, academic integrity, and the regulations of my university. Additionally, it was ensured that this usage was transparently disclosed and appropriately attributed.

Graz, December 2024 Lea Katharina Stursa

Disclosures

Parts of this thesis have already been published as an open access article under the terms of the Creative Commons Attribution-Non-Commercial License (CC-BY-NC), which permits use, distribution, and reproduction in any medium, provided that the original work is properly cited and is not used for commercial purposes.

Accuracy of Palatal Orthodontic Mini-Implants Placed Using Fully Digital Planned Insertion Guides: A Cadaver Study

Stursa L[1], Wendl B[1], Jakse N[1], Pichelmayer M[1], Weiland F[2], Antipova V[3], Kirnbauer B[1]

Journal of Clinical Medicine
Volume 12, 2023, 6782, ISSN 2077-0383
https://doi.org/10.3390/jcm12216782

[1] Department of Dental Medicine and Oral Health, Division of Oral Surgery and Orthodontics, Medical University of Graz, Graz, Austria
[2] Private Practice, Deutschlandsberg, Austria
[3] Division of Macroscopic and Clinical Anatomy, Gottfried Schatz Research Center, Medical University of Graz, Graz, Austria

All co-authors have approved the use of the data for the publication of this thesis.

Reproduced Figures and Tables from the publication are labelled with the citation (Stursa, L., Wendl, B., Jakse, N., Pichelmayer, M., Weiland, F., Antipova, V. and Kirnbauer, B. Accuracy of palatal orthodontic mini-implants placed using fully digital planned insertion guides: A cadaver study. Journal of Clinical Medicine, 2023.).

Acknowledgements

I would like to thank my supervisor, Univ.- Prof. Univ. FÄ Priv.- Doz. Dr. Brigitte Wendl, for her continuous support and encouragement throughout this dissertation and my orthodontic residency. I would also like to thank the other members of my thesis committee: PD DDr. Barbara Kirnbauer, who performed the surgical interventions in the study and provided invaluable advices. Ass.-Prof. Dr. Margit Pichelmayer, Univ.-Doz. Dr. Frank Weiland, Univ.-Prof. DDr. Norbert Jakse and Assoz. Prof. PD DDr. Michael Payer, who have all supported me continuously throughout this dissertation project.

I am grateful for the support of DI Irene Mischak and Philipp Tepesch, as well as the teams in the radiology and the orthodontics departments at the Department of Dental Medicine and Oral Health, Medical University of Graz, Austria.

I also would like to express my thanks to PD Dr. Björn Ludwig for his encouragement and Forestadent (Forestadent, Bernhard Förster GmbH) for providing the materials. Great thanks go to the Division of Macroscopic and Clinical Anatomy, Gottfried Schatz Research Center, Medical University of Graz, Graz, Austria, as this study would not have been possible without their support.

Finally, I would like to thank my family for their love and unwavering support - without you none of this would have been possible. I dedicate this dissertation to my family.

The doctoral thesis was conducted in the doctoral school “MUSCULOSKELETAL SYSTEM AND ORAL HEALTH”. This research received no specific grant from the Medical University of Graz, any funding agency in the public, commercial, or not-for-profit sectors.

Table of contents

Abbreviations and Definitions

ANOVA	Analysis of variance
CAD/CAM	Computer-aided design and computer-aided manufacturing
CBCT	Cone beam computed tomography
CEREC	Chairside Economical Restorations of Esthetic Ceramics
CEO	Chief executive officer
cm	Centimeter
Co-Cr	Cobalt-chromium
CT	Computed tomography
DICOM	Digital Imaging and Communications in Medicine
DLP	Digital light processing
e.g.	Exempli grata
FDM	Fused deposition modelling
GBG	Gingiva borne guide
ICC	Intraclass correlation coefficient
ICP	Iterative closest point
Max.	Maximum
Min.	Minimum
mm	Millimeter
Ncm	Newton centimeter
OMI	Orthodontic mini-implants
PJ	Photo jet
SD	Standard deviation
SLA	Stereolithography

SLM/SLS	Selective laser melting and sintering
SS	Stainless Steel
STL	Standard Triangle/Tessellation Language
TAD	Temporary anchorage device
TBG	Tooth borne guide
TPA	Transpalatal arch
UV	Ultraviolet
µm	Micrometer
3D	three-dimensional

List of Figures

List of Tables

Abstract

Objectives: Skeletal anchorage and digital workflows have become an integral part of orthodontic diagnosis and therapy, minimizing risk factors and treatment time with single-visit protocols. This study evaluated the transfer accuracy of fully digital planned, 3D printed surgical guides for orthodontic mini-implants (OMIs) compared with freehand insertion.

Material and Methods: Cone-beam computed tomography (CBCT) datasets and intraoral scans of the maxillae from 32 body donors were used to place 64 miniscrews in the anterior palate. The study involved three groups: two groups (A and B) used printed insertion guides, while in the third group (C) freehand insertion was performed. Postoperative CBCT datasets were superimposed with the planning model, to compare achieved OMI positions to the virtual target positions. Accuracy measurements were performed using dedicated orthodontic software, to detect angular and linear deviations in the miniscrew positions.

Results: Statistically significant differences were found for transverse angular deviations (4.81° in A vs. 12.66° in B and 5.02° in C, $p = 0.003$) and sagittal angular deviations (2.26° in A vs. 2.20° in B and 5.34° in C, $p = 0.007$). However, accurate insertion depth was not achieved in either guide group; while in group A insertion was shallower than planned (−0.17 mm), group B's insertion was deeper (+0.65 mm) than planned. Group B exhibited higher mean deviations between virtual and actual implant positions for both OMIs, both at the level of the implant head and tip. These differences were statistically significant ($p = 0.003$; $p = 0.0001$; $p = 0.008$) for OMI 1 (right) at the implant head (0.90 ± 0.37mm), and for OMI 2 (left) at the head level (0.96 ± 0.46mm) and at the OMI tip (1.43 ± 0.82mm). Preoperatively, all cases showed parallelism between OMI 1 and OMI 2, but none of the OMI pairs remained completely parallel. The deviation from parallelism was significantly ($p = 0.030$) higher in Group B (10.41° ± 7.29°) compared to Group A (5.19° ± 2.71°).

Conclusion: Digital planning of orthodontic mini-implants improves clinical predictability and ensures safety of adjacent anatomical structures. Hence, achieving high transfer accuracy is crucial. Despite showing slight deviations, guided insertion remains an accurate and safe method in clinical practice. Outsourcing the planning and fabrication of computer-aided design and computer-aided manufacturing (CAD/CAM) insertion guides proved beneficial for certain indications; showing superior accuracy compared with in-house–fabricated insertion guides.

Zusammenfassung

Ziel: Die digitale Planung und skelettale Verankerung sind ein wichtiger Bestandteil der kieferorthopädischen Diagnostik und Therapie. Ihre Anwendung trägt zur Minimierung von Risikofaktoren während der Behandlung und zur Reduzierung der Therapiedauer bei. Diese Studie untersuchte die Übertragungsgenauigkeit vollständig digital geplanter, 3D-gedruckter Bohrschablonen für kieferorthopädische Mini-Implantate (OMIs) und stellte diese Ergebnisse der freihändigen Insertion gegenüber.

Material und Methoden: Insgesamt wurden im Rahmen dieser Studie 64 Mini-Implantate, welche anhand von digitalen Volumentomographien (DVT) und Intraoralscans der Maxilla geplant wurden, im anterioren Gaumen von 32 Körperspendern positioniert. Die Studie umfasste 3 Gruppen: Zwei Gruppen (A und B) nutzten 3D-gedruckte Insertionsschablonen, während in der dritten Gruppe (C) freihändige Insertionen durchgeführt wurden. Postoperative DVT-Datensätze wurden mit dem digitalen Planungsmodell überlagert, um Abweichungen der Implantatpositionen zwischen geplanter und tatsächlicher Position zu untersuchen. Diese Abweichungen wurden mittels spezieller kieferorthopädischer Software vermessen, um Winkel- und lineare Abweichungen zu berechnen.

Ergebnisse: Es wurden statistisch signifikante Unterschiede für transversale (4.81° Gruppe A, 12.66° Gruppe B, 5.02° Gruppe C, p = 0.003) sowie für sagittale (2.26° Gruppe A, 2.20° Gruppe B und 5.34° Gruppe C, p = 0.007) Winkelabweichungen gefunden. In keiner der Gruppen konnte eine ideale Insertionstiefe erreicht werden; während die Insertion in Gruppe A nicht tief genug war (-0.17 mm), war die Insertion in Gruppe B tiefer (+0.65 mm) als geplant. In Gruppe B zeigten sich signifikante Abweichungen zwischen virtuell geplanter und tatsächlicher Implantatposition für beide OMIs. Diese statistisch signifikanten (p = 0.003; p = 0.0001; p = 0.008) Abweichungen wurden für das rechte Implantat (OMI 1) auf Kopfebene (0.90 ± 0.37 mm) und für das linke Mini-Implantat (OMI 2) auf Höhe des Implantatkopfes (0.96 ± 0.46 mm) sowie auf Höhe der Implantatspitze (1.43 ± 0.82 mm) gefunden. Präoperativ waren alle Mini-implantate parallel zueinander, während postoperativ keine exakte Parallelität der beiden Implantate nachweisbar war. Die Abweichung von der Parallelität war in Gruppe B (10.41° ± 7.29°) signifikant (p = 0.030) höher als in Gruppe A (5.19° ± 2.71°).

Schlussfolgerung: Durch die digitale Planung kieferorthopädischer Minischrauben und die anschließende Anwendung einer Bohrschablone kann die klinische Vorhersagbarkeit erhöht werden. Trotz geringer Abweichungen ist die geführte Insertion eine genaue und sichere

Methode, welche sich bereits im klinischen Alltag vieler Kieferorthopäden etabliert hat. In der vorliegenden Studie erwies sich die Auslagerung der Planung und Herstellung von CAD/CAM Bohrschablonen als vorteilhaft, da die kommerziell erhältlichen Bohrschablonen eine höhere Übertragungsgenauigkeit im Vergleich zu den in-house gefertigten Insertionsguides aufwiesen.

Introduction

Anchorage

In 1907 the term “anchorage” has been introduced to the orthodontic treatment by Edward Hartley Angle (1) and is defined as resistance to undesired tooth displacement (2). Anchorage is a limiting factor in orthodontics and its management is pivotal to obtain successful treatment results (3). Depending on the treatment objectives, the goal is to maximize desired tooth movements while unwanted side effects are to be minimized (3).

Anchorage situations

Traditionally there are three types of anchorage in the anteroposterior relation: minimum, moderate and maximum anchorage (2).
Further, there is absolute anchorage, meaning that the anchorage units remain completely stationary. In some indications, this kind of anchorage is necessary, but unfortunately, it is usually not achievable with traditional orthodontic mechanics. However, in the rare case of an ankylosed tooth, which distributes the applied forces to the surrounding bony structures, being part of the anchorage unit, absolute anchorage becomes attainable (2).

a. maximum anchorage: Maximum anchorage means that space (e.g., after premolar extraction) is closed by retraction of the incisors while the posterior teeth remain in their position. Maximum anchorage can be provided if the reactive force is completely neutralized (4).

b. moderate anchorage: Moderate anchorage is needed for reciprocal space closure, meaning that the space is closed with relatively equal movements of the anterior and posterior teeth (4).

c. minimum anchorage: Minimum anchorage is needed when the space closure should be achieved through mesial movement of the posterior segment whilst the anterior teeth maintain their position. There is only little neutralization of the reactive force (4).

Anchorage possibilities

There are various forms of orthodontic anchorage, such as other teeth, extraoral and intraoral appliances located at the palate, head, neck, cortical bone or implants in bone and its use should be considered in every treatment plan. Edward H. Angle already postulated in 1907 that the ideal anchorage would be an immovable base (5).

Anchorage can be reinforced in multiple ways, such as changing the position of the anchor teeth. Besides, the application of different bends in the wire can help to increase anchorage even more: Tweed and Begg introduced a distal inclination of molars (tip-back), Ricketts applied cortical anchorage for molars (in-out) and Burstone took advantage of a differential torque control (third order bend) (6).

As the gained anchorage from the aforementioned methods is often limited, auxiliaries are used to increase anchorage. There are intraoral and extraoral anchorage options available.

Intraoral anchorage

Every tooth has a certain anchorage value correlated to its root surface, thus when multiple teeth are connected these values accumulate (1). Anchorage can be enlarged by connecting multiple teeth to an anchorage block using a steel ligature (1).

To connect multiple teeth with rigid arches, such as a transpalatal arch (TPA) in the upper jaw or a lingual bar in the lower dentition, is theoretically a further option to strengthen anchorage. By the use of a TPA, anchorage is fortified, as a constant intermolar width can be maintained, leading to the molars engaging the buccal cortex during their anterior movement (7). However, Diar-Barkly et al. (8) concluded in their systematic review that a TPA alone does not provide sufficient anchorage for en-masse or two-step retraction cases when maximum anchorage is required. The Nance appliance, a modified version of the transpalatal bar including an acrylic button covering the anterior part of the palate, was introduced in 1947 (9). The support of the acrylic button on the palatal cortical bone is believed to reinforce anchorage (9). Diedrich et al. (6) cautioned against overrating the anchorage value of the Nance appliance and Al-Awadhi et al. (7) demonstrated that absolute anchorage could not be provided by its use.

To enlarge the anchorage unit, adding teeth from the opposing dental arch may be required (1). Intermaxillary elastics transfer the force to the other jaw, but unwanted side effects such as molar extrusion or tipping can occur (6).

Extraoral anchorage

The use of extraoral appliances, which are supported by extraoral patient's structures, like head and neck instead of teeth, can further increase the resistance of the anchorage unit. The most popular extraoral device is headgear, first mentioned by Kingsley in 1865. Today's headgear appliance goes back to Kloehns work in 1947 (10).

Traditionally a headgear consists of a facebow that is connected to teeth by molar bands and is anchored to the back of the head, through a head cap or neck strap (11). The desired force is created by elastic parts through the facebow and the reciprocal force is prevented by anchoring it against a stable structure, such as the back of the head (11). Headgear enables sagittal and vertical anchorage control and variation of the point of force application relative to the center of resistance of the maxilla allows for additional moment control (6). A Headgear needs to be worn at least ten to twelve hours for seven nights a week (12).

Extraoral support can also be provided by the wear of a facemask, with a forehead rest and a chin cup.

The major drawback of extraoral anchorage devices is that their success relies on patient compliance. According to Cole et al. (13) one third of the investigated patients reported their headgear usage not accurately. Hence it can be expected that patients report more headgear wear than actually performed (13). The success of most anchorage systems depends on patient compliance, which risks a prolonged treatment time or compromised treatment outcomes, if the patient doesn't cooperate (14). To overcome these issues associated with extraoral anchorage devices, a method using implants in the upper or lower jawbone has been introduced some decades ago (14). Wehrbein et al. (14) claimed that endosseous implants might be a useful alternative for stable intraoral anchorage.

Skeletal anchorage

In 1945 Gainsforth and Higley (15) recognized that anchorage gained from a point within the basal bone could greatly increase stability. They inserted vitallium screws in the mandibular ramus of six dogs and loaded them immediately to evaluate their ability of skeletal anchorage (15). All implants were lost because of loosening within a maximum of three weeks, most likely due to infection (15). They concluded that this method wasn't sufficiently stable for the duration of most orthodontic tooth movements (15).

Approximately 20 years later, in 1965, Linkow (16) demonstrated the use of implants as anchor for tooth movements and introduced the blade implant.
In 1969 Brånemark et al. (17) reported the long-term success of osseointegrated titanium implants in dogs, which were subsequently used in prosthetics in the following years.
Based on a study of a small sample of dogs Sherman et al. (18) concluded, that an implant cannot be moved by orthodontic forces, making it suitable for anchorage purposes.
In 1980 Turley et al. (19) investigated bilaterally inserted implants in the palate of monkeys for maxillary expansion.
A 15-year study by Adell et al. (20) reported that 89 - 100% of the titanium endosseous implants, used for edentulous rehabilitation, were still stable after 5-9 years.
Creekmore and Eklund (21) published a case report of upper anterior teeth intrusion in a class II division 2 patient using a vitallium screw, inserted just below the anterior nasal spine.
In 1984 a study performed on rabbits presented seven factors contributing to bony fixation of the implant and they concluded that titanium endosseous implants remain stable when loaded orthodontically (22). A healing period, in which the implant remains unloaded, of six weeks in rabbits, meaning four to five months in humans, is crucial to provide a good adherence from the bone to the implant surface (22).
Turley et al. (23) confirmed previous findings by showing that all investigated titanium endosseous implants, loaded with orthodontic or orthopedic forces, remained stable, indicating their potential as orthodontic anchorage units.
In 1990 Roberts et al. (24) presented a titanium implant used as rigid anchorage for intrusion and mesialization of a lower second and third molar, for the first time in a human.
The use of conventional prosthetic implants is not sufficient for orthodontic patients, often requiring different treatment schemes (14). Hence investigations of implant insertion in the palate (25) and the retromolar region (26) followed. Since bony structures in these regions differ from those in conventional implant regions, the geometry of the implants needed to be adapted (14). The idea of smaller, especially shorter implants was born and Wehrbein et al. (14) introduced “The Orthosystem” (Straumann, Basel, Switzerland) in 1996. The self-tapping titanium implant was available in 4 or 6 millimeters of length and presented a diameter of 3.3 millimeters (14). The surface was sandblasted and acid-etched to improve osseointegration (14). It was tested in six adult patients presenting a class II relationship and no implant dislocation under orthodontic load could be detected (14).

Endosseous implants serving solely as anchorage devices need to be removed after finishing orthodontic treatment (27). To avoid a second surgical intervention Glatzmaier et al. (27) introduced “BIOS”, a partially resorbable implant, which could not prevail.

In 1995 Block and Hoffmann (28) presented the “Onplant”, a thin titanium alloy disk with a hydroxyapatite coat that is inserted subperiosteally but does not have to be inserted into the bone. Hence it can be used at all stages of teeth eruption (28). Under local anesthesia a subperiosteal tunnel is prepared, to slide the “Onplant” into a position near the palatal midline and when osseointegration is achieved, the disk can be loaded (28).
Dental implants, the Orthosystem and the Onplant have a common characteristic, which is the prerequisite of osseointegration. Osseointegration refers to a direct, functional and enduring bond between vital bone and titanium implants, which is commonly achieved after a certain healing period (20).

Kanomi was the first to mention a temporarily placed miniscrew for orthodontic anchorage in 1997 (29). He used titanium miniscrew implants to intrude mandibular central incisors (29). The implants were placed between the root apices and loaded with intrusive forces (29).
In 1999 Park et al. (30) published a case report using titanium microscrews for distal movement of the whole maxillary dentition. Implants were loaded one month after insertion and remained stable and firm throughout the whole treatment (30).
In the same year Umemori et al. (31) introduced a temporarily implanted titanium miniplate, requiring intravenous sedation as it is a more extended surgical intervention than miniscrew insertion.

Various types of mini-implants have been invented since their first introduction, each presenting a different design or features. OMI’s can be placed before the treatment start, at the beginning or during treatment (32). They derive from maxillofacial fixation screws and usually present themselves smaller than the surgical screws (32).
In the literature, these anchoring elements can be found under a variety of names, such as mini-implants, micro-implants, miniscrews or temporary anchorage devices (TAD) (33).

Orthodontic mini-implants

OMI’s are temporary anchorage devices, meaning that they are fixed to bone for as long as anchorage reinforcement is required and are subsequently removed after use (34).

Mini-implants are made of titanium (35). Due to the formation of a passive oxide layer, pure titanium is biocompatible and practically inert (35). To achieve even better mechanical properties most orthodontic mini-implants are made from titanium alloy (Ti6AlV4, Titanium grade 5) (35).

OMI's are one-piece screws, consisting of three components, the implant shaft, transgingival area and the implant head (4).
The implant shaft, including the implant tip, with its thread is located within in the bone and anchors the implant (4). The design of the thread can be either self-drilling or self-tapping (35). Depending on the thread design, pilot drilling of the bone, according to the length and diameter of the implant, may be needed (35). Self-drilling implants can be screwed directly into the bone by using a screwdriver at an appropriate torque level (33).
The transgingival area is the connection between implant shaft and implant head and helps to prevent the penetration of pathological microorganisms (4). It is located in the mucosa (4).
There are different types of implant head designs available, such as hooks, balls or slots to enable a connection to orthodontic traction auxiliaries (4).
The implant length should be chosen according to the gingival thickness, wherein the ideal ratio of the screw outside the bone to the intraosseous screw part should be 1:1 (35). Since the gingiva sometimes reaches a thickness of 4 mm, the minimum implant length should be 8 mm (35). Miniscrews typically have a diameter ranging from 1.2 to 2.3 mm (4), but the susceptibility to implant fractures decreases with larger diameters (35).

Stability of orthodontic mini-implants is based on mechanical retention, which allows for easy removal and immediate loading of the implant (33). This makes them less technique sensitive than osseointegrated implants (33). Owing to the fact that the stability of the OMI relies on macroretention rather than osseointegration, good primary stability is requisite for the implant's success (36). The implant thread contributes to primary stability and osseointegration of mini-implants is largely prevented due to its mostly smooth surface, thus allowing for easy removal as soon as treatment goals have been achieved (37). Cortical bone quality and quantity are important factors contributing to primary stability (38).

Direct and indirect forces can be applied when using mini-implants (39). In indirect anchorage cases a group of teeth, onto which an orthodontic force is applied, are stabilized against the mini-implant, hence the implant is loaded indirectly (40). Direct anchorage is provided, when traction is applied to the head or abutment of the mini-implant (33).

Insertion sites – anterior palate

Orthodontic mini-implants perforate soft tissues as well as hard tissues since they are inserted transmucosally and anchored intraosseously (41). For most indications the anterior palate is the preferable insertion site for OMI use in the upper jaw, as it combines attached gingiva,

adequate cortical bone supply and sufficient distance to dental roots (41). The surrounding bone volume is fundamental for the success of mini-implants, whether inserted buccally or in the palate (42).

The anterior palate and its bone quantity and quality have therefore been studied thoroughly since the Orthosystem has been introduced by Wehrbein et al. (43) in 1996. Wilmes et al. (44) defined a T-shaped area directly posterior to the palatal rugae, encompassing the anterior palate and the midpalatal suture, as the “T-Zone” and declared it as a suitable region for safe OMI insertion due to the amount of bone and its superior quality. Ludwig et al. (42) found a palatal bone height of 7.3 ± 3.1 mm in an area 3-4 mm from the distal aspect of the incisive foramen median in the suture and 3 mm paramedian a bone height of 8.3 ± 0.8 mm. Another study found a mean bone thickness of only 2.94 mm at the palatal suture and suggested OMI insertion 6-9 mm distal to the incisive foramen and 3-6 mm paramedian to the suture (45). As it is not easy to accurately identify the incisal foramen clinically, Baumgaertel et al. (46) suggested interproximal tooth contacts as reference points and found bone thickness of 8.7 ± 2.3 mm between canine and first premolar at 2 mm paramedian. The location of contact points is influenced by tooth movements and by tooth morphology and hence seems not to be ideal as reliable reference point (47), but the palatal rugae was found to remain stable over time and thus was recommended as landmark during orthodontic treatment (48). Hourfar et al. (47) found bone depth of 7.6 - 8.1 mm at the level of the third palatal rugae and concluded that the most distal palatal rugae is a stable and easily identifiable anatomical landmark for OMI insertion.

For median and paramedian placement, 30° to 20° tipping to the posterior at anterior locations and anterior tipping of -30° at posterior median and paramedian positions yielded the best bone support (49).

According to Wilmes et al. (44) OMIs can be inserted either median or paramedian, whereas median insertion is applicable for sagittal and vertical tooth movements and paramedian OMI positioning is recommended for rapid maxillary expansion and sagittal or vertical tooth movements. If TADs are inserted in a sagittal direction (median insertion) along an anteroposterior line, an interscrew distance of 7-14 mm should be applied and if transverse OMI insertion (paramedian insertion) is performed, an interscrew distance of 5-10 mm is recommended (44). In children and growing adults an intrasutural insertion (median insertion) should be avoided to prevent possible negative effects on growth and development (50). Hence, TAD insertion in growing patients in the paramedian area is deemed the safer choice

to impede interactions with possible remaining intermaxillary suture growth changes in the transverse plane (50).

The quality and thickness of the palatal gingiva play an important role when it comes to successful mini-implant insertion as the OMIs pass through the soft tissue (42). Thinner attached gingiva is considered advantageous for OMI placement as the likelihood of inflammation is lower (51). Soft tissue measurements at the area of the midpalatal suture revealed that the thickest part was 4 mm posterior to the incisive papilla and remained uniformly thick 1 mm posterior to this point (52).

Success rates

Several factors adversely have an impact on the success of mini-implants (53). Among these are an improper insertion depth (54), clinician experience (55), incorrect insertion angle (56) or an unfavourable insertion site (41).

The systematic review of Mohammed et al. (57) investigated the role of anatomical sites and correlated risk factors on the survival of OMIs. An overall failure rate, for the three palatal insertion sites, of 4.7% was found, with a failure rate of 1.3% for mid-palatal, 4.8% for paramedian and 5.5% for parapalatal insertion (57).

Arqub et al. (58) published overall success rates for mini-implants of 79.5%, with a success rate of 91.5% for palatal insertion. Of the investigated maxillary buccal TADs 77.1-82.6% were successful, while mandibular buccal insertion only had a success rate of 68.3-70.4% (58).

Another study investigated a total of 384 paramedian miniscrews and found an overall success rate of 97.9%, indicating an outstanding survival rate (59). Excellent performance of the OMIs, used for rapid palatal expansion (98.0%) and distalization (97.8%), could be shown in this study (59).

Success rates of implants placed in the infrazygomatic crest vary between 71.9-93.7% (60, 61). Chang et al. (62) found success rates of 93% for mini-implants inserted in the buccal shelf area, while the 24-month success reported by Arqub et al. (58) was only 20.8%. Infrazygomatic crest and buccal shelf screws are often related with discomfort due to their insertion in the movable mucosa (63).

Hong et al. (64) concluded that the stability of OMIs placed in the mandible is 2.23 times lower than in the upper jaw.

The highest success rates and hence the most reliable outcomes were found for miniscrews placed in the anterior palate (91.5- 98.9%) (58, 65).

According to Arqub et al. (58) the intended purpose of the mini-implant and the magnitude of forces have a significant influence on the success rates. They found high survival rates for molar protraction and molar intrusion, probably due to the low magnitude of force required for intrusion and the high bone quality of the bone stock in the anterior insertion region (58). Further observations revealed that the 12-month survival rates for distalization were significantly lower (58). Additionally, to the bone quality and the applied force levels, bad oral hygiene could have led to these findings (58).

Risk factors / Complications

Complications may occur during the insertion, orthodontic treatment and during the removal of the mini-implant. According to Baumgaertel et al. (66) OMIs perforate the gingiva, the periosteum, the cortical and cancellous bone, and often lie close to dental roots in a normal insertion. Consequently, the mini-implant interacts with both the hard and soft tissues, which must be taken into account when attempting to place a miniscrew in a specific region (67).

Studies have shown that proximity of the OMI to the dental roots can decrease implant success (68, 69), but it is unlikely that long-term damage will occur to the dental roots (70).
Asscherickx et al. (71) reported that in beagles, after accidentally damaging the tooth roots, nearly complete repair of the cementum could be attained within a period of 18 weeks. Initial repair occurred at the earliest 12 weeks after implant removal (71).
Kim et al. (70) found that cementum repair on the affected root surfaces occurred as soon as the contacting mini-implants were removed and any resulting trauma was repairable if continuous contact with the root was prevented.
A study using scanning electron microscopy, investigating the impact of intentional contact between the root and OMI on root surfaces, revealed that the main part of root surface restoration occurred eight weeks after implant removal or the applied orthodontic forces (72). Two premolars had accidental direct contact with the screws, indicating a high risk of injury, given that only twenty OMIs were investigated (72).
Lee and colleagues (73) demonstrated that even in cases where root perforations involved the pulp and resulted in root fracture, self-repair of the root was possible. Invasive treatment

options, including root canal treatment, were not required for root regeneration upon immediate miniscrew removal (73).
Mini-implants have been monitored throughout orthodontic loading and it was found that they migrate up to 0.4 mm, indicating that OMI's do not remain absolutely stationary like an endosseous implant (74). According to Liou et al. (74) a minimum distance of 2 mm between the root surface and the OMI should be present to prevent root damage. With a periodontal ligament width of approximately 0.25 mm, a 1 mm clearance between the OMI and the root is considered appropriate for the preservation of a healthy periodontium and ensuring mini-implant stability (75). Hence, if the available space in the interradicular area is at least 3.5 mm, insertion of mini-implants with a diameter of 1.5 mm is deemed safe (75).

Sinus perforation, including both the maxillary and nasal sinuses, can occur when placing mini-implants in the anterior or posterior maxillary regions as well as in zygomatic regions (76). According to Brånemark et al. (77) and Ardekian et al. (78) immediately loaded dental implants that perforated the nasal or maxillary antrums showed no difference in implant stability. Orthodontic miniscrews perforating the maxillary sinus do not require immediate removal, due to their small diameter (76). Continuation of the treatment is possible if the patient is observed for potential development of sinusitis or mucocele (76). Motoyoshi et al. (79) found out that 10% of the investigated miniscrews perforated the maxillary antrum, yet perforations $\leq$1.5 mm in depth rarely influence screw stability.

Trauma to blood vessels can result in bleeding, which can be challenging to control, in particular if it affects the palatine vessels (80). Fäh et al. (81) reported one case of prolonged secondary bleeding after palatal OMI insertion. Prolonged bleeding can usually be stopped with compression and if compression fails, constriction of the bleeding vessel can be attemped using a suture or electrocautery (81).

During OMI insertion in the palate, mandibular buccal dentoalveolous and retromolar region there is a risk of nerve injuries (76). Most minor nerve injuries, excluding complete tears, are transient, normally resolving within 6 months, while persistent sensory abnormalities may require interventions such as pharmacotherapy, microneurosurgery, laser therapy or grafting (82).

Guided OMI Insertion

To help achieving a favorable implant position for dental implants, the use of a surgical guide was introduced more than 30 years ago (83). The idea is that their application helps optimizing the use of available bone, while lowering the risk of trauma to adjacent anatomical structures during dental implant insertion (84).

OMIs are typically inserted freehand without guidance (85), but Cousley et al. (86) introduced a surgical guide for mini-implants. The common objective of orthodontic surgical templates is to impede trauma to anatomical structures and diminish patient discomfort, as well as to prevent implants from being inserted beyond the target insertion depth and reproduce the planned insertion angle (87).

Early surgical guides were often wire guides transferring the 2-dimensional information from radiographs to the surgical site, aiming to facilitate the insertion process (88). In 2000 Bernhart et al. (45) transferred the ideal OMI position found on a dental CT to the respective patient intraoperatively by means of a curved caliper. Subsequently, Martin et al. (89) presented a vacuum-formed guide having a hole at the intended insertion site, yet this delivered positional information only. Hence a transfer of preplanned angular information was not possible with this design (89).

In 2002 a 3-dimensional surgical guide with an integrated drill sleeve was used to minimize errors in implant placement and aiding intraoperatively to choose the correct inclination of the implant long axis (90). A vacuum formed stent with an integrated metal stent at the insertion site, providing positional and angulational information was introduced (90). Following, many CT or CBCT based surgical templates were proposed (91, 92, 93) and in 2016 Maino et al. (87) were the first to fuse a lateral cephalogram with an intraoral scan for mini-implant position planning and template fabrication.

Initially drill templates were laboratory-factored using vacuum-formed foils (89), resins (90) or silicones (84), while today surgical guides are often 3D printed (87, 91) or milled (94) using CAD-CAM technology.

The planning of guided insertion can be undertaken with various different orthodontic software programs, either utilizing cone-beam computed tomography or a lateral cephalogram and a digital intraoral scan (95). Various studies on virtual OMI position planning were published, some combining impressions and CBCT images (92, 96) others using a lateral cephalogram and impressions (84, 87), CBCT and intraoral scans (97), lateral cephalograms and intraoral scans (95, 98) or only using a CBCT without dental model (99). When the “appliance first” concept is practiced, the orthodontic appliance itself serves as an insertion aid (100). Hence

the mini-implants are inserted only after the device itself has been placed, without the need for an additional surgical template (100).
The fusion of a CBCT dataset and an intraoral scan for designing a surgical guide, can help to accurately determine the point of insertion of the OMI in the mucosa and to determine the direction of the mini-implant (97). Acrylic resin surgical templates fabricated on dental casts, without radiological superimposition, can provide information of the point of insertion but not of the OMIs inclination and pathway through the bone (97).

Even though digital workflows and their clinical implementation are complex and implicate a steep learning curve, printed devices have shown high accuracy and minimal error rates (101). The precision of fully guided OMI insertion can be affected by numerous factors (102). Parameters such as template production, intraoral scanning, accuracy of the 3D printer, radiographic inaccuracies, as well as matching and template fit during insertion, may evoke inaccuracies in the clinical process (102). According to the systematic review of Jung et al. (103) no statistically significant differences concerning the different methods for template fabrication were found among the investigated studies. Casetta et al. (91), Möhlhenrich et al. (84) and Ludwig et al. (53) investigated the transfer accuracy of different insertion guides.

The simultaneous digital fabrication of the insertion guide and a corresponding orthodontic appliance allow for a 1-visit protocol and hence chair time can be reduced, which is a benefit for the patient, the clinician and the office agenda (95). Among the additional benefits mentioned are the increased patient comfort and enhanced treatment efficiency (101). The use of insertion guides instills a sense of security to unexperienced clinicians and can help to achieve a higher success rate (55). Templates potentially reduce the hesitation towards mini-implant application, as the execution of surgical interventions can cause uncertainties for some specialized orthodontists (55). Simultaneous insertion of the OMIs and the corresponding appliance enable a precise fit, thereby reducing the risk of implant overloading and accordingly minimizing the risk of implant failure (101). Using an insertion guide, mini-implants are placed at the correct depth and parallel insertion of multiple miniscrews is possible (87). It allows for sufficient penetration in the bone but prevents a too deep insertion with soft tissue compression, if a built-in depth stop is used (55). The surgical template facilitates an uninterrupted, continuous insertion from the beginning to the planned insertion depth, which is advantageous in preventing a significant increase in material stress and avoiding implant fracture (55).

Digital workflow / CAD-CAM planning

Digital technologies and workflows were first integrated into dental offices in 1974, when computerized scheduling systems were introduced (104).

The rapid progress in computer-aided design software, 3D printers, surface and volume scanners and the widespread use of CBCTs have significantly affected the field of digital orthodontics throughout the last years (105). A typical overall digital workflow in dentistry includes three primary processes: the acquisition of digital information, the processing of this data and the application in the clinical environment (106). A successful implementation of the digital workflow requires both hardware components and dedicated software for analyzing STL models and other digital files (107).

Early in the beginning of the digital revolution, orthodontic software was employed to digitize and store all patient records (105). The first dental CAD software was developed in 1985 by Mörmann and Brandestini, who introduced the Chairside Economical Restorations of Esthetic Ceramics (CEREC) system (105). At the present, the main task of a digital software is creating a virtual patient out of all available digital documents (108). These software tools are available as open-source, freeware, or proprietary solutions (101). 3D data from skeleton, dentition and facial soft tissues are accessible, however the issue of merging these different data formats, as DICOM format for CBCT or STL (Standard Tessellation Language) for intraoral scans, endures (109). Using dedicated software programs these datasets can be superimposed to create the virtual patient for further planning steps (110). The voxel-based, surface-based and point-based superimposition methods exist (109). Marker-based superimposition relies on easily identifiable reference points that can be recognized on 3D radiographs (111). Surface-based superimposition describes an automatic fusion procedure, based on selected surfaces that are aligned by an iterative closest point (ICP) algorithm (109). For the point-based registration, which is a direct and semi-automatic procedure, a minimum of three consistent landmarks are manually chosen on both 3D objects and subsequently the “least squares” method aligns the 3D objects according to the best fit for the point couples (109).

With intraoral optical scanning technology, the creation of precise virtual surface models of the teeth and gums is now possible, presenting an accurate alternative to conventional impressions (112). The virtual design of orthodontic devices relies on gathering intraoral information of the patient, using an intraoral scan or digitized conventional plaster models (101). Further processing, like mesh repair and hole filling, of the STL file of the digital model is needed to create an appliance (101).

Due to the rapid evolution of the CBCT toward extremely low radiation doses and its excellent spatial resolution, diagnosis has improved and the 3D environment can be used for planning purposes (112). Nevertheless, the use of standard lateral cephalograms for orthodontic surgical template creation results in reduced costs and minimizes radiation exposure (87). The suitability of using a lateral cephalogram for paramedian insertion was confirmed in a study of Kim et al. (113), who showed that the bone height measured on the lateral x-ray corresponds with those 5mm paramedian. This method is appropriate for the majority of patients for determining the ideal positions of OMIs, with CBCTs mainly necessary in cases involving impacted teeth, unerupted upper incisors or narrow maxillae (84). Particularly in cleft patients the advantages of a more accurate and reliable insertion of the mini-implants compensate for the increased costs and radiation exposure linked with the CBCT (84).

After superimposition of radiograph and digital model, a desired orthodontic device can be digitally designed or the position of OMIs can be planned using a dedicated software (114).
Virtual mini-implant placement is carried out according to clinical guidelines on the digital model, followed by displaying the x-ray to optimize the OMI position in relation to bone supply and anatomical neighboring structures (55). Once the ideal virtual mini-implant position is defined, the surgical guide can be produced directly or indirectly (110). While for the indirect method, an additional physical model for the placement of insertion sleeves is necessary (114), the direct method uses rapid prototyping without the need for an analog intermediate step (110). In the direct method, the insertion guide, ideally including a depth stop, can be designed within the orthodontic software program (55) and subsequently transformed into physical form through 3D printing (114).
3D printing, also referred to as additive manufacturing, describes the process of creating complex and individual objects by depositing a certain material in consecutive layers (115). The 3D designed object is sliced into digital cross-sections and is transmitted to the 3D printer (116). Insertion guides and dental models are typically printed using particular resin materials (101) and can be categorized into light-curing and fused deposition modelling (FDM) (117). Three main light curing technologies are used for printing photosensitive resins: stereolitography (SLA), digital light processing (DLP) and photo jet (PJ) (101). While in SLA and DLP, objects are made from a reservoir of liquid resin that is selectively exposed to UV light, in PJ technology resin micro drops are sprayed onto a platform, which cure simultaneously via UV light (101).
In 2017 Graf et al. (118) were the first to publish a 3D printed metal appliance for orthodontic use. 3D metal printing is another type of additive manufacturing, in which 3D metal objects are built based on a sequential layering technique using metal powder (116). Metal orthodontic

appliances are typically fabricated by selective laser melting and sintering (SLM/SLS), known as bed powder fusion (105), and if needed, hooks or tubes can be added to the printed appliance by welding them to the framework (101). The printed appliance exhibits support structures after 3D printing, which need to be removed for a smooth surface (110). The majority of metal printed orthodontic devices are made from Cobalt-Chromium (Co-Cr) alloys, although stainless steel (SS) and titanium are also available (105). Any printed object intended for intraoral use that may come into direct contact with blood, must be sterilized before use (101).

With the use of digital technologies, the orthodontic workflow becomes more efficient, as the manufacturing steps can be minimized, which results in reduced error rates and increased precision (116). Nevertheless, the success of digital planning relies on the expertise and experience of the operator, as the superimposition, the digital placement of the virtual implants, and the design and manufacturing of the surgical guide are error-prone (55). The design and manufacturing process of such devices can also be outsourced to external companies if desired (110).

Justification of the research question

Digital technologies have established themselves both in general dentistry and in the orthodontic field in recent years. The application of dedicated software programs and the wide availability of 3D technologies enable the fabrication of customized appliances and transfer guides for OMI insertion. The fully digital preoperative planning for mini-implant positioning and the design of individualized appliances has also been made accessible to a wide range of orthodontists, including those in private practices.

While there is a plethora of publications on mini-implants, recent research investigating surgical guides is becoming more common, although with a majority being case reports. While these case reports present the technique of a surgical guide, an evaluation of the actual achieved results of the digital planning is often lacking.

Nevertheless, further information on the accuracy levels of the transfer of such digitally planned implant positions is still missing. Additionally, the question whether there are differences between freehand and guided mini-implant insertion arises and it would be interesting to determine whether the effort involved in the digital planning and printing process of insertion guides is justified. Another interesting aspect that has not yet been sufficiently studied is the deviations from the planned positions at different OMI segments (OMI head and tip). A further noteworthy question pertains to whether the design of the insertion guide has an impact on the level of transfer accuracy.

Aims of the dissertation

The primary aim of the study is to investigate two fully digital planned insertion guides for orthodontic mini-implant insertion and to assess their precision and reliability, to determine if one method may be used preferably. These achieved positions are examined using angle and distance measurements.

The data gathered during the course of this study allow for comparison with conventional OMI insertion, which is a secondary aim of the study.

Another secondary objective of this study is the examination of the parallelism of the two mini-implants relative to each other.

Hypotheses

For this purpose, the following null hypothesis and respective alternative hypotheses have been identified:

Null-Hypothesis

H_0: There are no statistically significant differences in the transfer accuracy between the two investigated insertion guides, both fabricated within a purely digital workflow.

Alternative Hypotheses

H_1: There are statistically significant differences in insertion depth between the used insertion guides.

H_2: There are statistically significant differences in the transfer accuracy measured at the implant head between the used insertion guides.

H_3: There are statistically significant differences in the transfer accuracy measured at the implant tip between the used insertion guides.

H_4: There are statistically significant differences in the transfer accuracy between left and right mini-implant.

H_5: The use of insertion guides for OMI insertion does not allow for significantly higher parallelism in the transverse and sagittal planes compared with freehand insertion.

Materials and Methods

Study design and ethical approval

Ethical approval was obtained from the Ethics Committee of the Medical University of Graz (EK 32-550 ex 19/20). While alive, all body donors had given their informed consent for the donation of their postmortem tissues for research purposes. All body donors were bequeathed to the Division of Macroscopic and Clinical Anatomy of the Medical University of Graz (Austria) under the approval of the Anatomical Donation Program of the Medical University of Graz and in accordance with the Austrian laws concerning body donations.

Following insertion criteria were defined as the following:

- Intact palatal gingiva
- No impacted or displaced teeth
- No syndromes or cleft-lip-palate
- At least two remaining teeth in quadrants I and II

Following exclusion criteria were defined:

- Damaged palatal gingiva
- Impacted or displaced teeth
- Syndromes, cleft-lip-palate
- No two-point support because of less than two remaining teeth in quadrants I and II

The study involved heads from 32 individuals provided by the Division of Macroscopic and Clinical Anatomy of the Medical University of Graz, with intact palatal gingiva, embalmed using a modified Thiel technique (119). These body donor skulls were randomly split into three groups:

- Group A (n=12): commercially available 3D printed insertion guide (Accuguide®; Forestadent Bernhard Förster GmbH, Pforzheim, Germany)
- Group B (n=12): selfdesigned, individually adapted 3D printed insertion guide
- Group C (n=8): no surgical guide, freehand conventional insertion

Record acquisition and digital planning

The initial records included a CBCT dataset of the upper jaw (Planmeca Promax 3D Max®, Finland) with dimensions of 10 x 9.3 cm (diameter x height) and a voxel size of 200 µm, along with an intraoral surface scan of palate and teeth, which was performed for each body donor head using the Trios3® (3Shape, Copenhagen, Denmark) intraoral scan.

The obtained DICOM (digital imaging and communications in medicine) data and the surface STL (standard triangulation language) file of each skull belonging to group A were uploaded to the encoded professional planning portal (Forestadent Bernhard Förster GmbH). The digital planning of the OMI position was performed by a renowned, international TAD expert (B.L.) and pioneer in digital dentistry. We received a digital positioning proposal and after our approval, the 3D printed insertion guides and the corresponding 3D resin-printed models were sent to us.

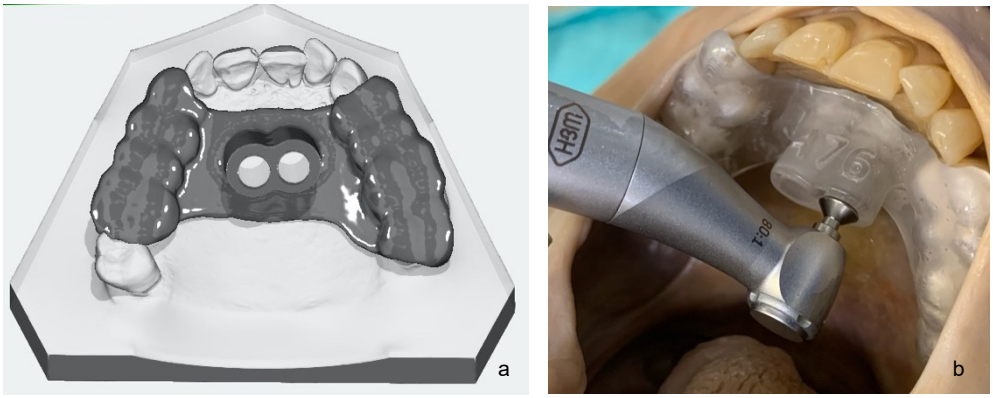

Figure 1: Insertion Guide – Group A. a. digitally planned insertion guide (accuguide®) b. insertion process with the accuguide® in situ[1]

In group B superimposition and digital planning of the insertion guide were performed by one experienced orthodontist (L.S.) using the dedicated orthodontic software program OnyxCeph (Image Instruments GmbH, Chemnitz, Germany). The DICOM dataset and the STL file were uploaded into the software as 3D objects. Before adding the DICOM dataset of the CBCT to the object list, it was necessary to convert it into a surface rendering model. Therefore, the threshold for hard tissue needed to be defined to represent real conditions at the planned implant area. Within the module extension “Register 3D” a fusion model of the two datasets was created, by superimposing the CBCT dataset and the intraoral surface scan model. To register both objects correctly, corresponding surface points on both models had to be selected and afterwards superimposition was performed by a best-match algorithm. At least three

[1] Figure 1b. published as Figure 2(c) in Stursa, L., Wendl, B., Jakse, N., Pichelmayer, M., Weiland, F., Antipova, V. and Kirnbauer, B. Accuracy of palatal orthodontic mini-implants placed using fully digital planned insertion guides: A cadaver study. Journal of Clinical Medicine, 2023.

different corresponding dental surface points were chosen for precise superimposition. A 3D model containing hard and soft tissues was the result of the merging of datasets and it was further loaded into the module “TADmatch”.

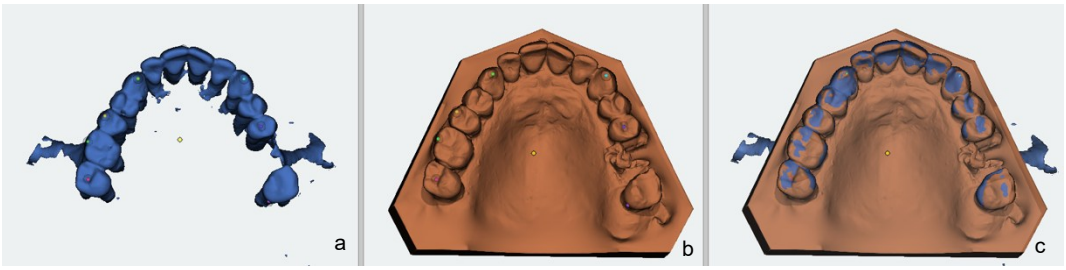

Figure 2: Superimposition based on corresponding surface points (green) a. CBCT dataset b. intraoral scan dataset c. fusion model of both datasets

In the module TADmatch the desired TAD type was chosen from a virtual library where various TADs from different manufacturers are available. The plan was to virtually insert two parallel OrthoEasy® Pal (1.7 × 8 mm; Forestadent Bernhard Förster GmbH) mini-implants with an interscrew distance of 6 or 7 mm in a paramedian position. The pair of virtual miniscrews was placed by using a cursor that allowed movements of the virtual TADs in all three planes, choosing an ideal paramedian position at an angle of about 90° to the palatal plane. Subsequently, the merged CBCT was displayed and the chosen implant positions were adjusted based on bone availability, root proximity, nerves and blood vessels.

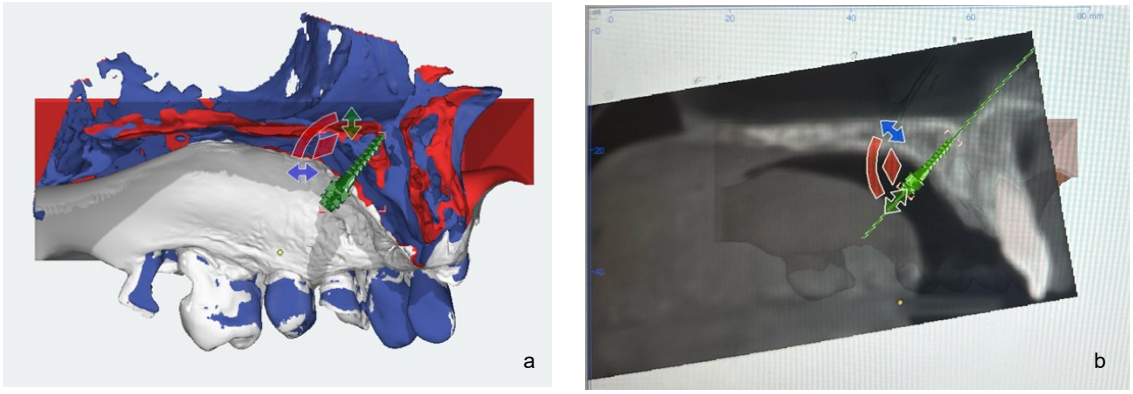

Figure 3: Virtual implant placement a. OMI placement using the 3D cursor for all planes b. OMI placement with superimposition of the CBCT dataset

As the final position of the OMIs was defined, a positioning model was created and its STL data was transferred to another dedicated software program (Appliance Designer®, 3Shape,

Copenhagen, Denmark), where the responsible dental technician (P.T.) and the orthodontist (L.S.) virtually designed the surgical guides. The surgical guide was designed to enable a tilt-free positioning through dental support in the posterior region of the left and right sides of the maxilla. The drilling templates lie on the occlusal surfaces of the remaining teeth and the length of the drilling channel was chosen as a depth stop during insertion.

These templates were printed via a light processing technique (Asiga Pro2®, Dentona, Germany) and subsequently light hardening (Otoflash G171®, Dentona, Germany) with 2 times 2000 flashes was executed under the presence of Nitrogen (N2). A biocompatible resin (Optiprint Gide 385®, Dentona, Germany) with a layer thickness of 0.075 mm (75 µm) was used and the applied printer software was Asiga Composer Version 1.2.8. The attempt was to create a surgical guide that is reduced in size, presenting a more skeletonized shape compared to former insertion guides.

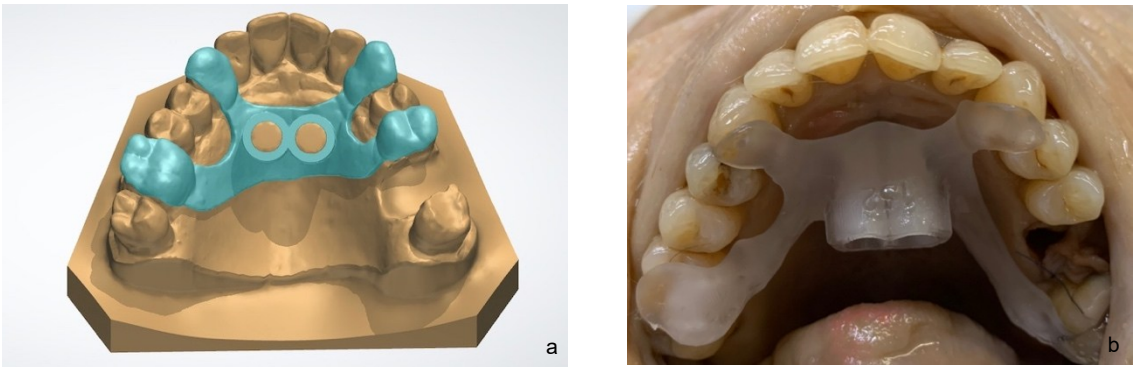

Figure 4: Insertion guide – Group B. a. digitally planned, selfdesigned insertion guide b. 3D printed insertion guide in situ[2]

In group C intraoral surface scans and CBCTs were obtained and studied by the very experienced oral surgeon (B.K.) before TAD insertion, but no special digital presurgical planning has been carried out.

[2] Figure 4b. published as Figure 2(b) in Stursa, L., Wendl, B., Jakse, N., Pichelmayer, M., Weiland, F., Antipova, V. and Kirnbauer, B. Accuracy of palatal orthodontic mini-implants placed using fully digital planned insertion guides: A cadaver study. Journal of Clinical Medicine, 2023.

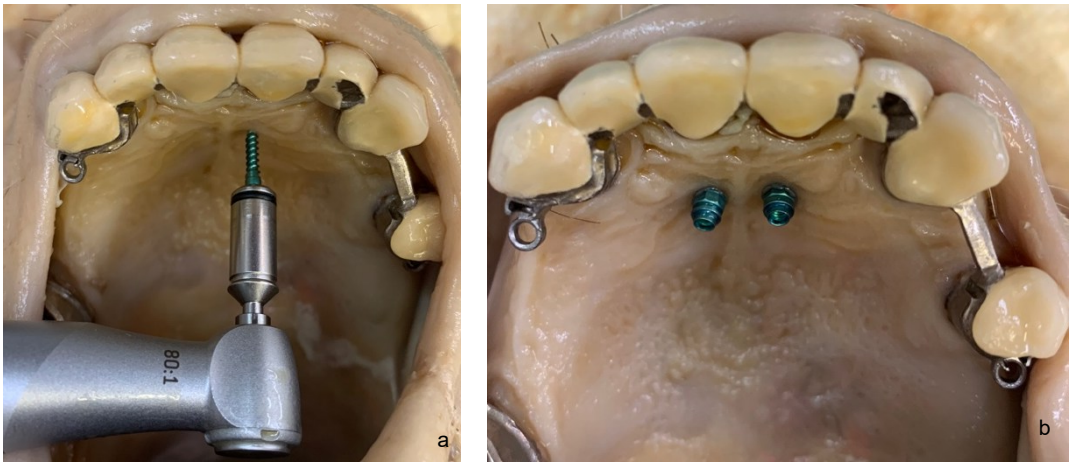

Figure 5: OMI insertion – Group C. a. freehand insertion b. OMIs in situ[3]

OMIs and drill blade

In the present study, OrthoEasy® Pal (Forestadent, Bernhard Förster GmbH) mini-implants with a length of 8 mm and a diameter of 1.7 mm were used. Two mini-implants were inserted per cadaver maxillae, resulting in a total of 64 OrthoEasy® Pal mini-implants used in this study.

Mini-implant insertions were performed using the corresponding insertion blades, provided by Forestadent. These blades serve as a connector between the handpiece and the OMI, and their outer diameter was considered in the design of the drilling template. As soon as the appropriate depth for the mini-implant insertion is reached, the blade contacts the upper edge of the surgical guide, functioning as an integrated depth stop (Fig.7).

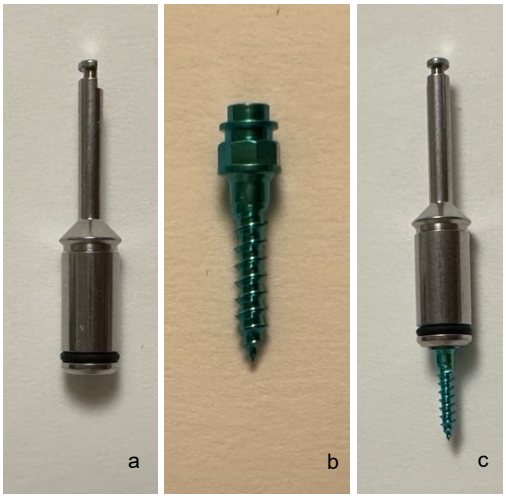

Figure 6: OMI insertion tools a. drill blade b. Forestadent OrthoEasy® Pal Mini-implant c. OMI inserted in drill blade

[3] Figure 5a. published as Figure 2(d) in Stursa, L., Wendl, B., Jakse, N., Pichelmayer, M., Weiland, F., Antipova, V. and Kirnbauer, B. Accuracy of palatal orthodontic mini-implants placed using fully digital planned insertion guides: A cadaver study. Journal of Clinical Medicine, 2023.

Surgical procedure

During OMI insertion the surgical guides were positioned on the teeth and held in position by an assistant (L.S.) while one well-experienced oral surgeon (B.K.) performed the insertions. All insertion procedures were performed by the same oral surgeon using the right hand. In group C OMI insertion was performed conventionally, free handed as normally done in clinical routine. OMI 1 was always positioned right, OMI 2 left of the palatal suture.

A contra-angle cordless handpiece drive (Prosthodontic implant driver, W&H, Bürmoos, Austria) with a corresponding screwdriver (Forestadent, Bernhard Förster GmbH) was used for OMI insertion. The insertion was performed without predrilling, as OrthoEasy® Pal TADs are self-drilling and self-tapping, in all groups. Insertion torque was limited to 35 Ncm and a drilling speed of 25 turns per minute was set. In groups A and B, where surgical guides were applied, the insertion stopped automatically as the Forestadent screwdriver contacted the top edge of the insertion guide.

Figure 7: Automatic insertion stop using the Forestadent drill blade[4]

Postsurgical data acquisition and accuracy measurements

Postoperatively a CBCT (Planmeca Promax 3D Max®, Finland) scan, with a voxel size of 200 µm and dimensions of 10 x 9.3 cm (diameter x height), of each cadaver head was performed and matched with the corresponding preoperative planning data using the Register3D® tool (OnyxCeph, Image Instruments GmbH). Additionally in six cadaver heads, so in three specimens of each surgical guide group, a scanbody abutment (Forestadent, Bernhard Förster GmbH) was applied onto the OMI head and intraoral surface scans using the Trios3® (3Shape) were performed.

[4] Figure 7. published as Figure 2(c) in Stursa, L., Wendl, B., Jakse, N., Pichelmayer, M., Weiland, F., Antipova, V. and Kirnbauer, B. Accuracy of palatal orthodontic mini-implants placed using fully digital planned insertion guides: A cadaver study. Journal of Clinical Medicine, 2023.

For accuracy measurements a further superimposition of the preoperative OMI position (STL dataset of preoperative planning model) and the actual OMI positions (surface rendering models originating from postoperative CBCTs) were needed. The preoperative planning datasets (STL) of Group A were given to us by Forestadent. All virtual OMIs were marked with points at the implant head and tip. The tip of OMI 1 (right) was marked as point “4” and the head was point “1”, for OMI 2 (left) the tip was defined as point ”3” and the head was point “2”. These measurement points were set personally by Dr. Tom Kühnert, CEO of OnyxCeph.

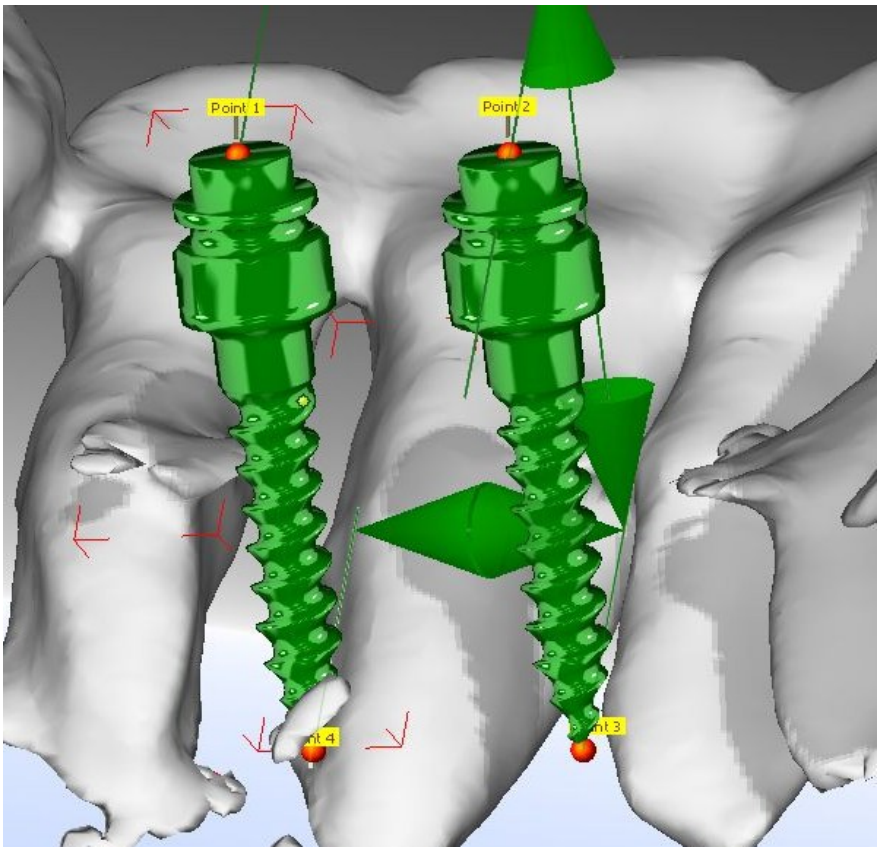

Figure 8: Measurement points 1-4

For group A and B the preoperative planning model was uploaded into the module “Register 3D” and then the surface rendering model of the postoperative CBCT was added to the object list. The datasets were superimposed using the point-to-point function for corresponding dental reference points on both models. Once these datasets were aligned, superimposition of virtual and actual mini-implants was performed using automatic surface registration by an iterative closest point (ICP) algorithm. Superimposition of virtual and actual TAD positions was

performed three times by one single well-experienced orthodontist (L.S.). By superimposing the actual mini-implants with the virtual OMIs, it was possible to obtain the exact coordinates for the actual head and tip measurement points.

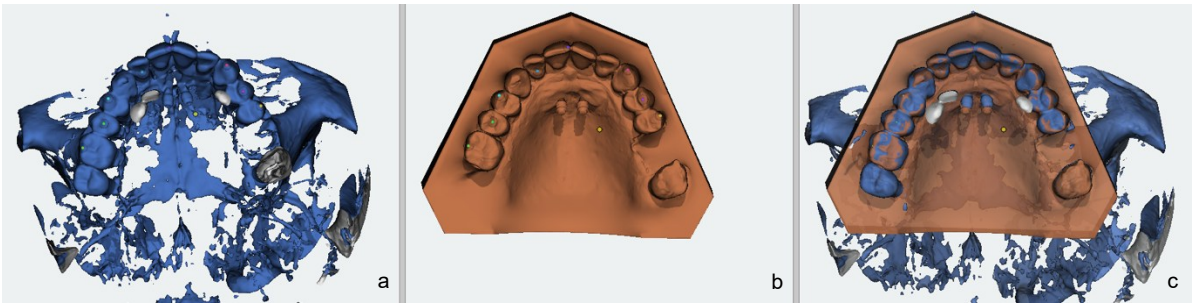

Figure 9: Superimposition (c) of postoperative CBCT dataset (a) and preoperative planning model (b) using the point to point function

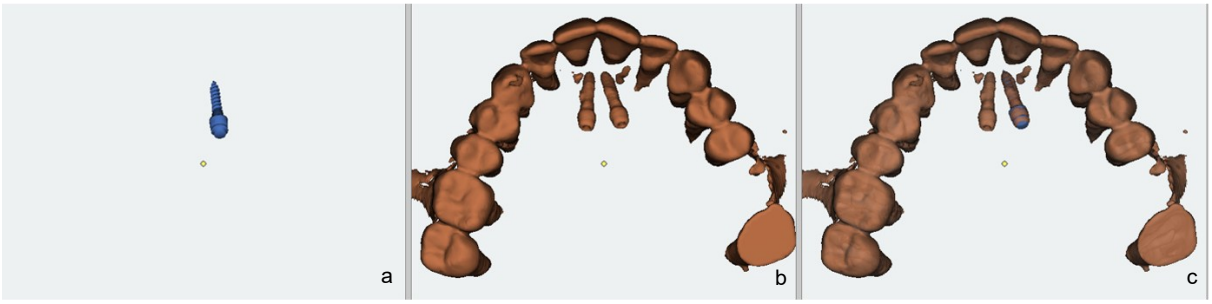

Figure 10: Superimposition (c) of virtual OMI (a) into the CBCT dataset (b)

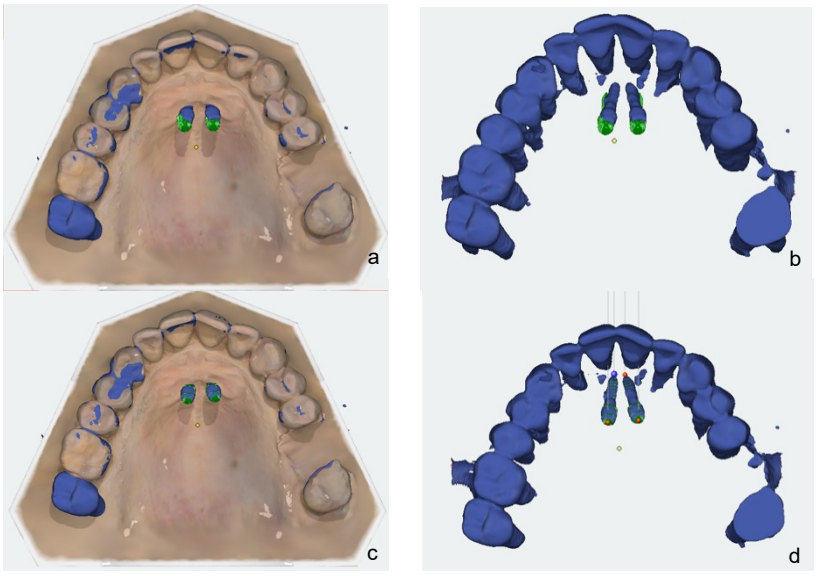

Figure 11: a. + b. after superimposition of pre- and postoperative datasets

c. + d. after superimposition of virtual TADs into actual TAD positions

The exact coordinates of the four points pre- and postoperatively were extracted, using the “export function” provided by OnyxCeph within the module “Digitize 3D”. These coordinates were collected in an Excel spreadsheet and subsequently calculations for linear and angular deviations were performed. Linear measurements were undertaken to evaluate insertion depth and to measure deviations and interscrew distances at the level of the implant head and tip. With the angular measurements parallelism of the OMIs and their deviations compared to the preoperatively planned positions were investigated. As postoperative superimposition was performed three times, mean coordinates were used for measurements and calculations. Deviations were defined at the center of the implant head, at the implant tip and along the long axes of the OMIs.

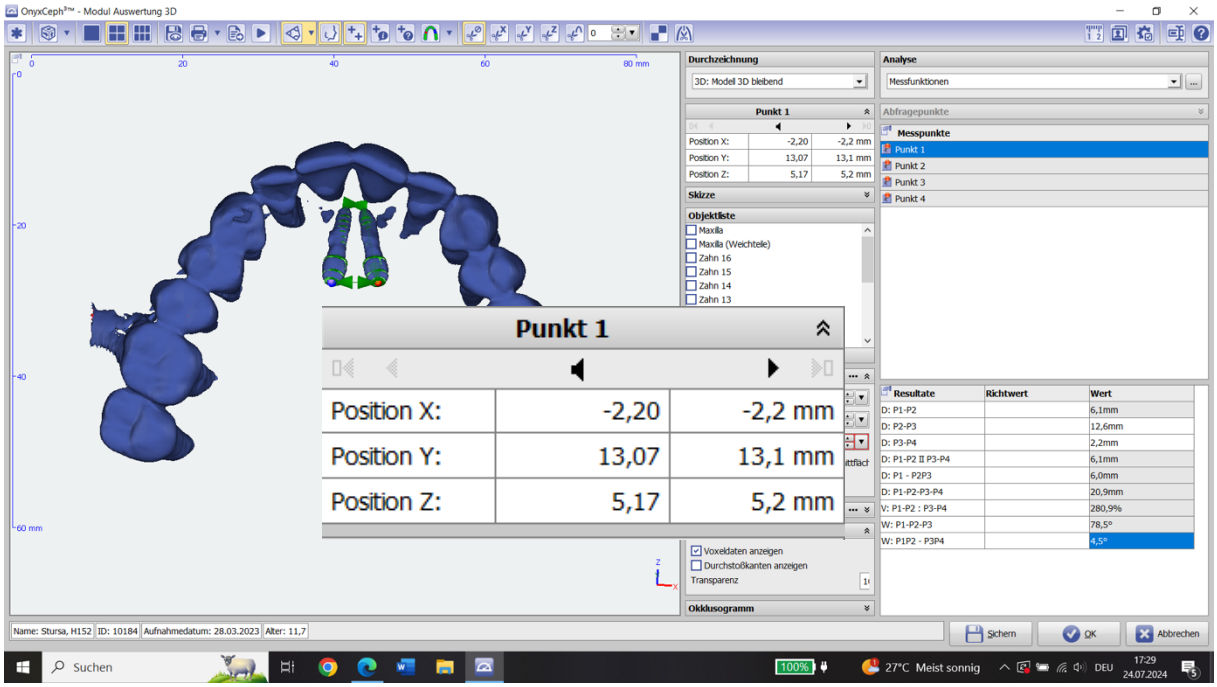

Figure 12: OnyxCeph “Digitize 3D” module – extraction of coordinates for each point (1-4)

In group C no preoperative virtual OMI positions were available, but accuracy measurements were possible for angular deviations in a transverse and sagittal point of view. These measurements were performed directly in the CBCT software (Romexis, Planmeca, Finland). The axis of OMI 1 was parallel transitioned until a point of intersection with the long axis of OMI 2 was reached, and the angle between these two axes was measured. Angular measurements were performed using the “Digitize” module (OnyxCeph, Image Instruments, Chemnitz, Germany).

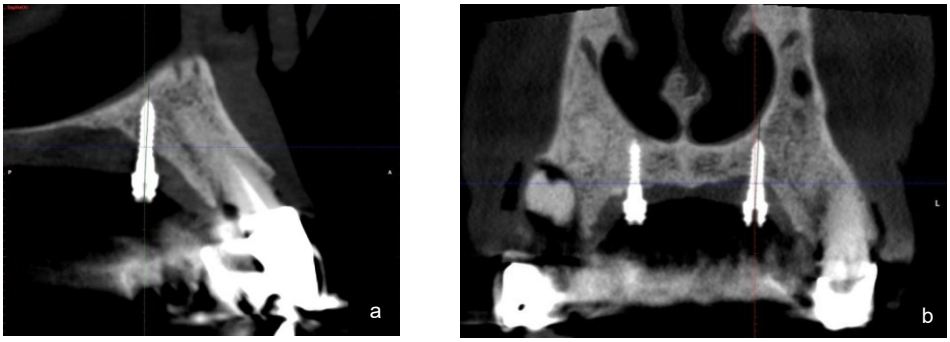

Figure 13: a. sagittal angular measurements (green axis - OMI 1, black axis - OMI 2)
b. transverse angular measurements (red axis - OMI 1, black axis - OMI 2)

For six specimens a postoperative intraoral surface scan using scan bodies was performed. Two scanbodies were screwed onto the head of the OMIs in each case and silicon was put in between the scanbody and the palatal surface to allow for an intraoral surface scan without errors. The obtained STL files were uploaded into the OnyxCeph library and opened in the “Register 3D module” where a superimposition with the preoperative planning model was conducted, to ensure the same 3D orientation of the datasets. Subsequently another superimposition with virtual scanbodies was conducted to display the four measurement points at OMI tip and head. Superimpositions were again performed using the ICP-Algorithm. Their coordinates were exported to perform linear and angular measurements and compare it to CBCT outcomes.

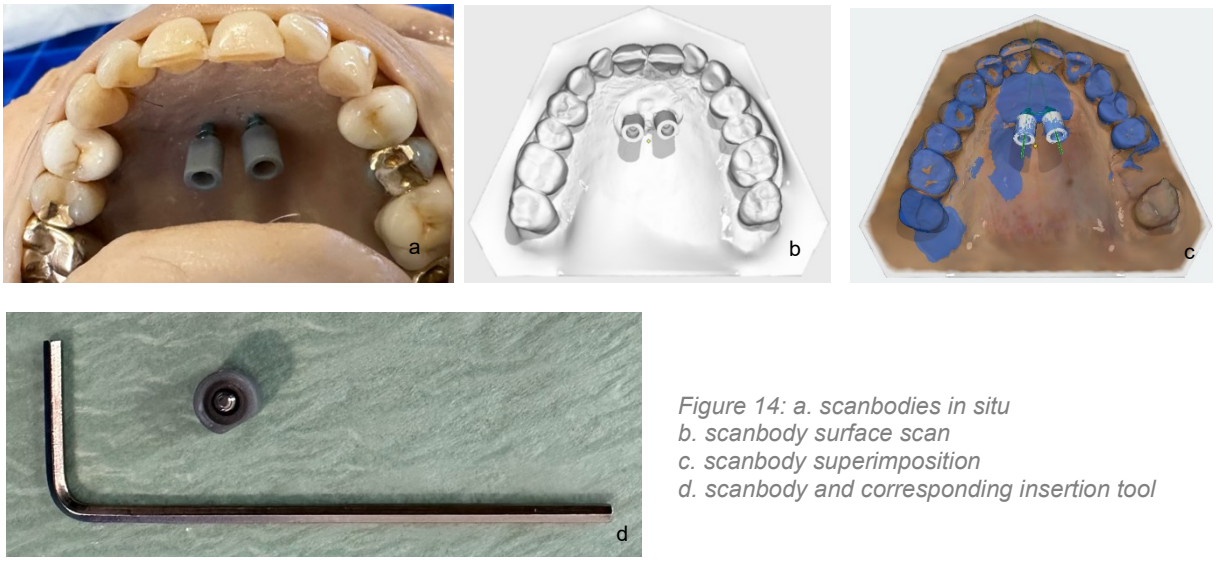

Figure 14: a. scanbodies in situ
b. scanbody surface scan
c. scanbody superimposition
d. scanbody and corresponding insertion tool

To calculate deviations at the level of the OMI tip and head we used the distance formula for vectors:

$$d = \sqrt{(a_1 - b_1)^2 + (a_2 - b_2)^2 + (a_3 - b_3)^2}$$

The deviations were indicated in mm. Interscrew distance (pre and post), insertion depth, deviations at the implant tip and head were investigated.

To obtain the angle between those vectors and to calculate angular deviations the following formula was used:

$$\varphi = arccos\left(\frac{\vec{a}\cdot\vec{b}}{\sqrt{\vec{a}}\cdot\sqrt{\vec{b}}}\right)$$

To calculate the shortest distance between two skew lines, the common normal vector to the two direction vectors is obtained using the cross product:

$$\vec{n} = \vec{a} \times \vec{b}$$

The distance between the skew lines is derived from the dot product:

$$d = \frac{\left|(\vec{a} - \vec{b})^{\circ}\vec{n}\right|}{|\vec{n}|}$$

Different axial deviations were investigated, namely interscrew parallelism (right OMI and left OMI post) and angular deviations of the planned and actual OMI axes (right OMI pre versus post; left OMI pre versus post). Results were listed in °. The alignment of the coordinate system was defined by OnyxCeph and the surface scan model.

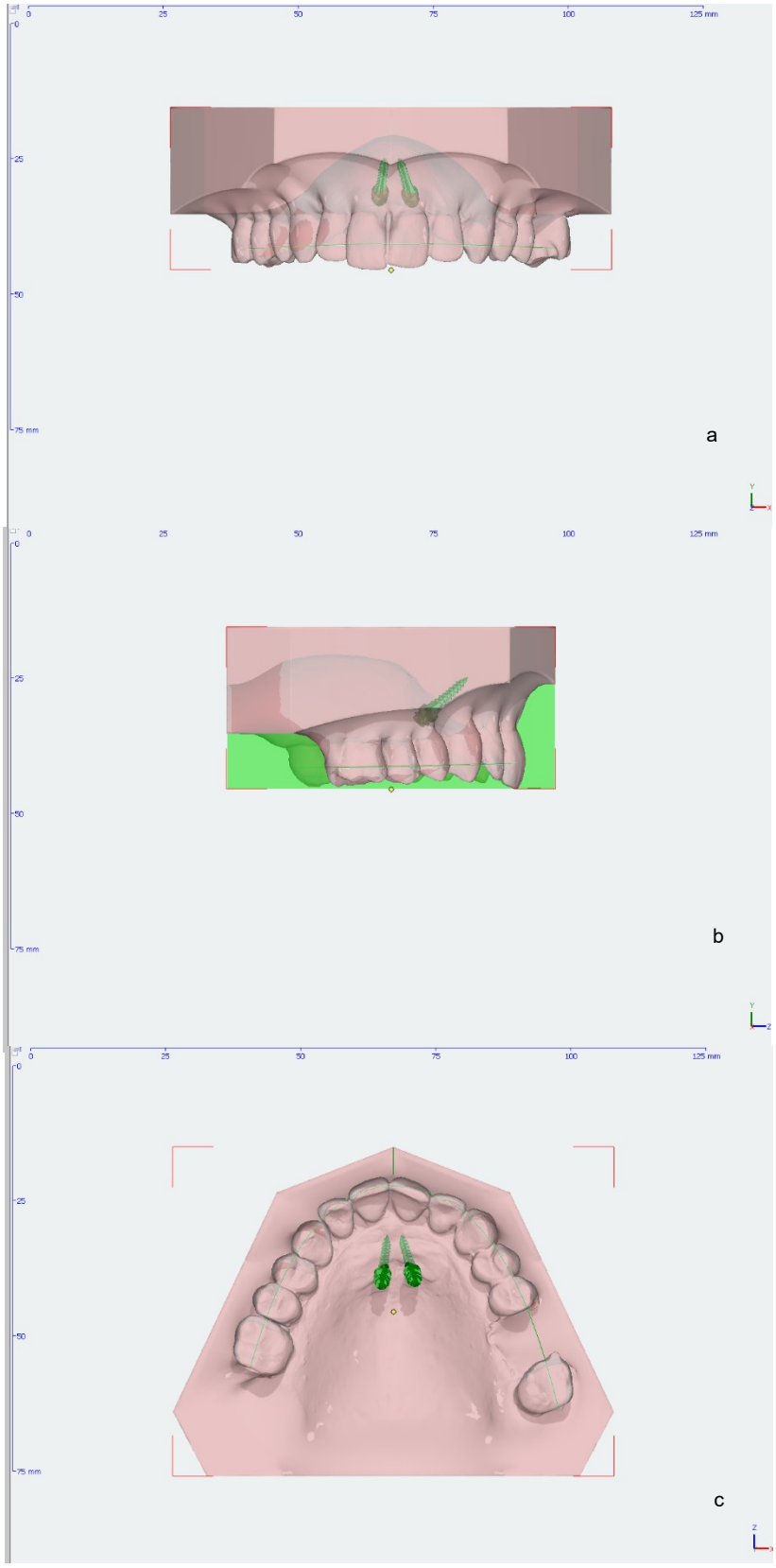

Figure 15: a. projection onto the frontal plane (z=0) – transversal deviations

b. projection onto the sagittal plane (x=0) – sagittal deviations

c. projection onto the occlusal plane (y=0) – vertical deviations

Statistical methods

Statistical analysis was performed using the statistical software package SPSS version 27.0 (IBM SPSS statistics, IBM Corporation, Armonk, New York, NY, USA).

With a sample size of 12 in each of the two main groups the study has a power of 87.71% to detect a difference in means of -0.4 (the difference between a Group 1 mean, μ_1, of 0.56 and a Group 2 mean, μ_2, of 0.96) assuming that the common standard deviation is 0.3 using a two group t-test with a 5% two-sided significance level.

Continuous variables are given as means ± standard deviations, maximum (Max.) and minimum (Min.) deviations were calculated and indicated. The independent students t-test was used to compare TAD position data and ANOVA was performed for comparison of the three groups. The level of significance was set at $p \leq 0.05$.

Results

Group A and B (measurements in three-dimensional space)

OMI parallelism of OMI 1 and OMI 2, pre versus postoperative

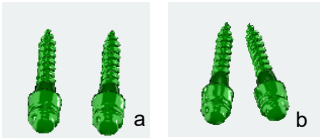

Figure 16: a. parallel OMIs b. deviation in OMI parallelism

pre: OMIs (1 and 2) were always parallel (both groups)

post: OMIs (1 and 2) were never parallel (both groups)

The amount of deviation from parallelism can be assessed with the angle:

	Min	Max	Mean	SD	p*
Group A	1.50	10.70	5.19	2.71	p = 0.030
Group B	2.31	22.77	10.41	7.29	

*Table 1: OMI parallelism (°) measured as angles between OMI 1 and OMI 2 (*t-test for individual samples)*

Preoperatively parallelism between OMI 1 and OMI 2 was given in all cases in both groups, postoperatively none of the investigated OMI duos showed parallelism. The deviation from parallelism was measured as angles between both implant axes, which presented to be significantly (p = 0.030) larger in group B (10.41° ± 7.29) than in group A (5.19° ± 2.71).

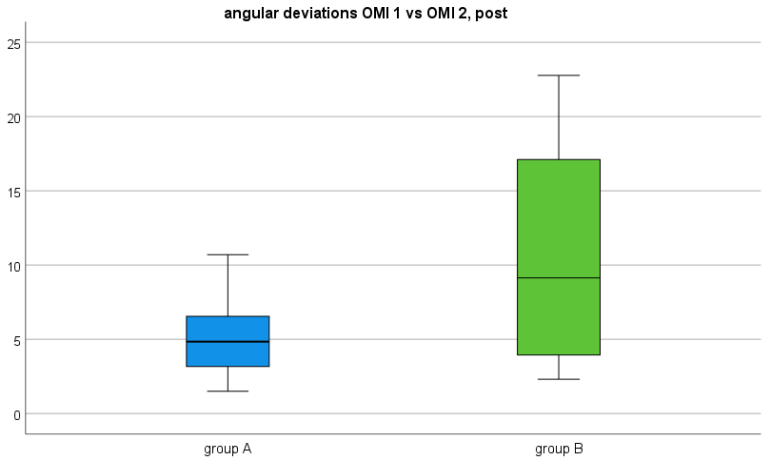

Figure 17: Postoperative angular deviations (°) from OMI parallelism in both groups measured as angles between implant axes of OMI 1 and OMI 2.

Axial deviation OMI 1 versus OMI 2 – pre versus post, group A and B separately

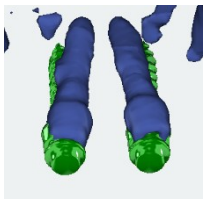

Figure 18: blue - actual position, green - planned position

		Min	Max	Mean	SD	p*
OMI 1	Group A	1.15	7.97	4.68	1.77	p = 0.720
	Group B	0.64	13.79	5.13	3.93	
OMI 2	Group A	0.83	10.36	4.07	3.13	p = 0.206
	Group B	0.49	22.60	6.66	6.13	

Table 2: Axial deviations (°) between planned and actual positions of OMI 1 and OMI 2 in both groups (t-test for individual samples).*

Concerning the axial deviation of the planned and actual OMI position no significant (p = 0.720 OMI 1, p = 0.206 OMI 2) difference between left and right OMI could be found in both groups. In group A the angular deviation was higher for OMI 1 (4.68° ± 1.77) and in group B OMI 2 showed a higher deviation (6.66° ± 6.13).

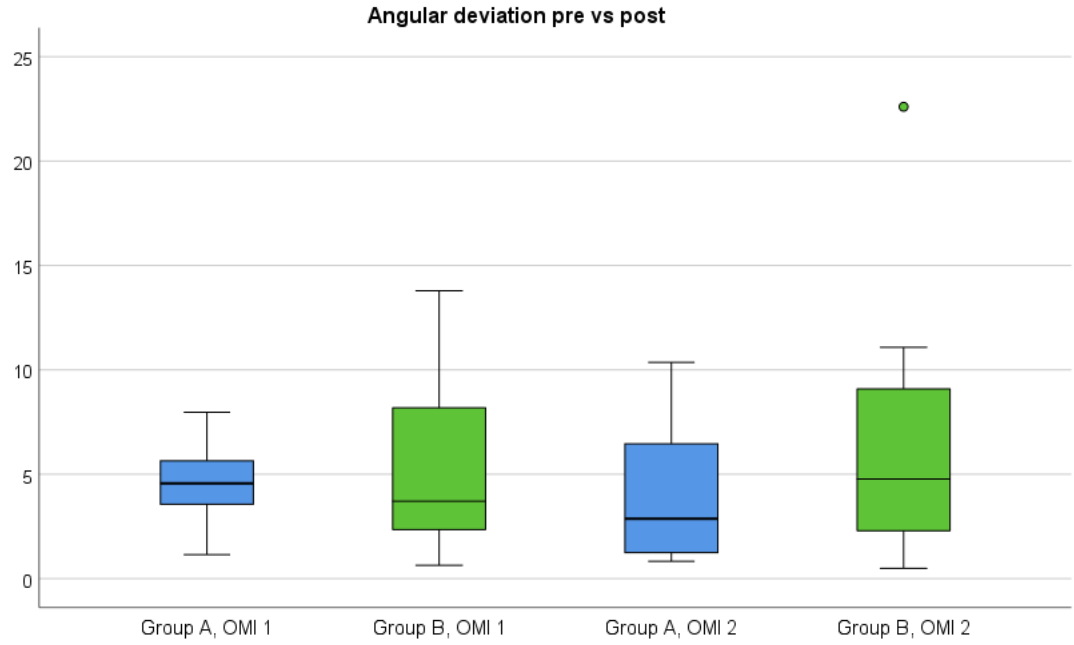

Figure 19: Angular deviations (°) between planned and actual positions of OMI 1 and OMI 2 in both groups.

Axial deviation OMI 1 versus 2 – pre versus post, group A and B combined

	Min	Max	Mean	SD	Sign. p*
OMI 1	0.64	13.79	4.90	2.99	p = 0.698
OMI 2	0.49	22.60	5.36	4.94	

Table 3: Axial deviations (°) between planned and actual positions of OMI 1 and OMI 2 - both groups summed up.

When group A and B were summed up to investigate angular deviations between planned and actual implant axes no statistically significant (p = 0.698) difference was found. In total OMI 2 showed a slightly higher axis deviation (5.36° ± 4.94) compared to OMI 1 (4.90° ± 2.99).

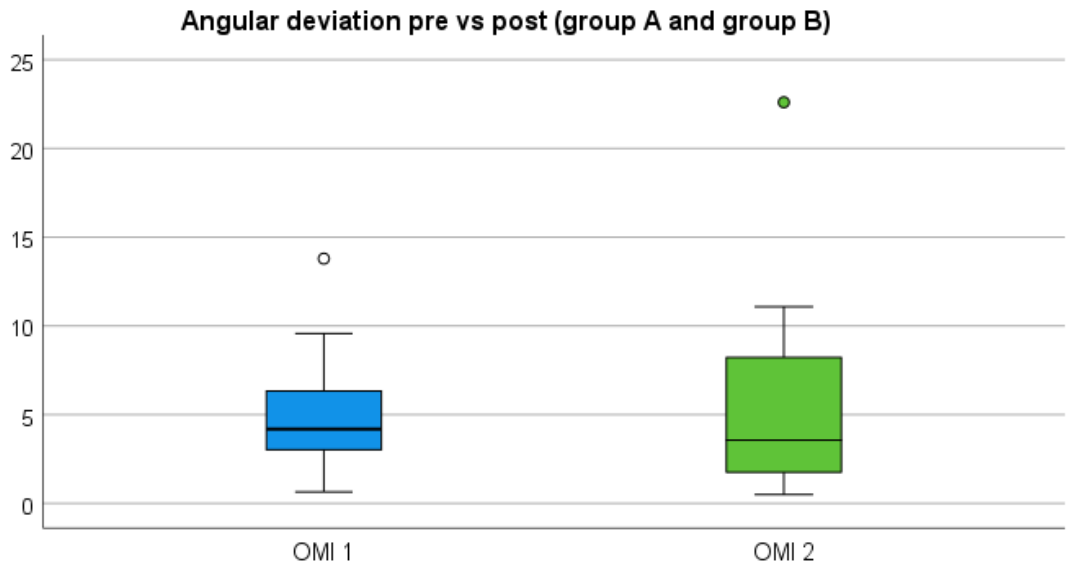

Figure 20: Axial deviations (°) between planned and actual positions of OMI 1 and OMI 2 - both groups summed up.

Interscrew distance OMI 1 and OMI 2, pre versus post

Figure 21: Interscrew distance measured at head and tip levels

Interscrew distance		Min	Max	Mean	SD	p*
head pre	Group A	6.00	7.00	6.83	0.39	p = 0.557
	Group B	6.00	7.00	6.92	0.29	
tip pre	Group A	6.00	7.00	6.83	0.39	p = 0.557
	Group B	6.00	7.00	6.92	0.29	
head post	Group A	5.78	7.09	6.71	0.46	p = 0.895
	Group B	6.13	7.64	6.74	0.39	
tip post	Group A	4.61	7.83	6.41	1.10	p = 0.719
	Group B	2.16	10.12	6.12	2.57	

Table 4: Interscrew distances (mm) measured at the implant tip and head pre- and postoperatively (t-test for individual samples).*[5]

Mean interscrew distances were measured at the level of the implant tip and implant head. In both groups the actual interscrew distance became smaller compared to the planned OMIs, however this was without significant differences (p = 0.557; p = 0.557; p = 0.895; p = 0.719).

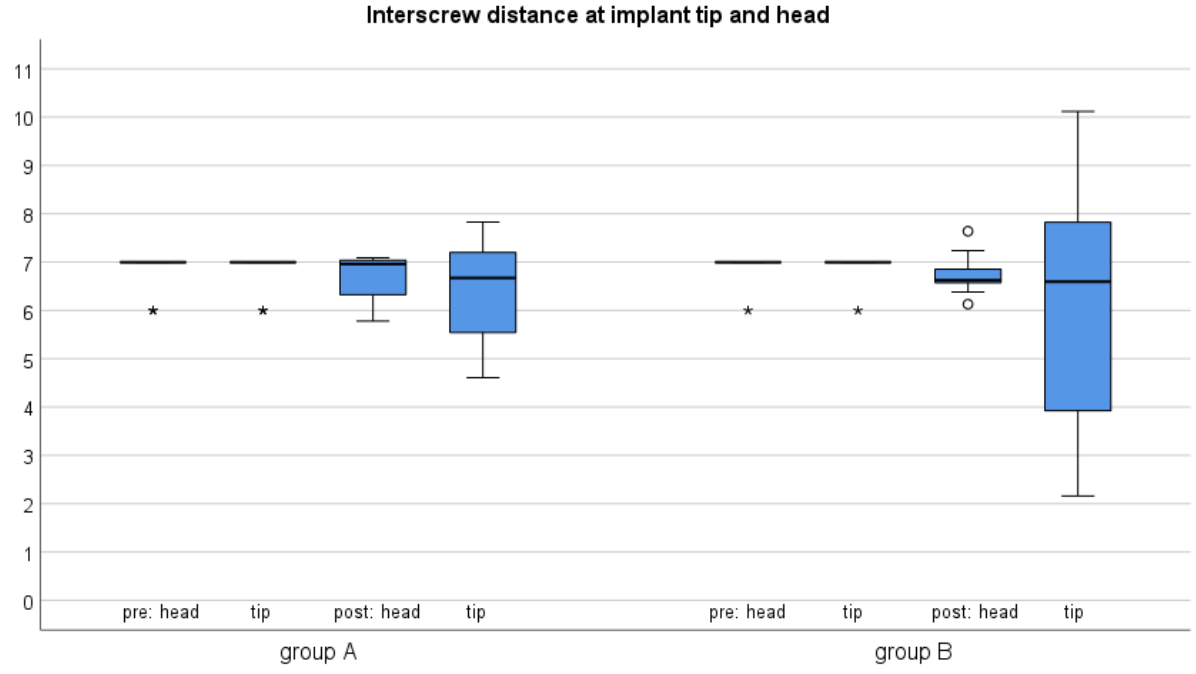

Figure 22: Interscrew distance (mm) measured at the implant head and tip pre- and postoperatively in Group A and B.[5]

[5] Figure 22. published as Figure 4. & Table 4 published as Table 1 in Stursa, L., Wendl, B., Jakse, N., Pichelmayer, M., Weiland, F., Antipova, V. and Kirnbauer, B. Accuracy of palatal orthodontic mini-implants placed using fully digital planned insertion guides: A cadaver study. Journal of Clinical Medicine, 2023.

Deviations pre versus post – OMI 1 and OMI 2 separately

distance pre - post		Min	Max	Mean	SD	p*
OMI 1 head	Group A	0.05	1.11	0.60	0.31	p = 0.003
	Group B	0.25	1.59	0.90	0.37	
OMI 1 tip	Group A	0.18	2.05	0.87	0.43	p = 0.091
	Group B	0.20	3.34	1.17	0.76	
OMI 2 head	Group A	0.24	1.14	0.56	0.28	p = 0.001
	Group B	0.18	1.83	0.96	0.46	
OMI 2 tip	Group A	0.27	2.22	0.87	0.55	p = 0.008
	Group B	0.56	3.96	1.43	0.82	

Table 5: Coordinate deviations (mm) between pre- and postoperative OMI positions measured at the head and tip level for OMI 1 and OMI 2 in each group.[6]

Deviations between pre- and postoperative coordinates measured at the head and tip of both OMIs showed significant differences between the two groups. Coronal deviations (head level) for OMI 1 showed significantly (p = 0.003) bigger deviations in group B (0.90 ± 0.37 mm) than in group A (0.60 ± 0.31 mm). The head level of OMI 2 showed also significantly (p = 0.001) higher discrepancies for group B (0.96 ± 0.46 mm) compared to group A (0.56 ± 0.28 mm). The deviations measured at the tip (apical deviations) of OMI 2 presented significantly (p = 0.008) lower deviations in group A (0.87 ± 0.55 mm) than in group B (1.43 ± 0.82 mm). Only apical deviations of OMI 1 were without significant (p = 0.091) differences in group A (0.87 ± 0.43 mm) and group B (1.17 ± 0.76 mm).

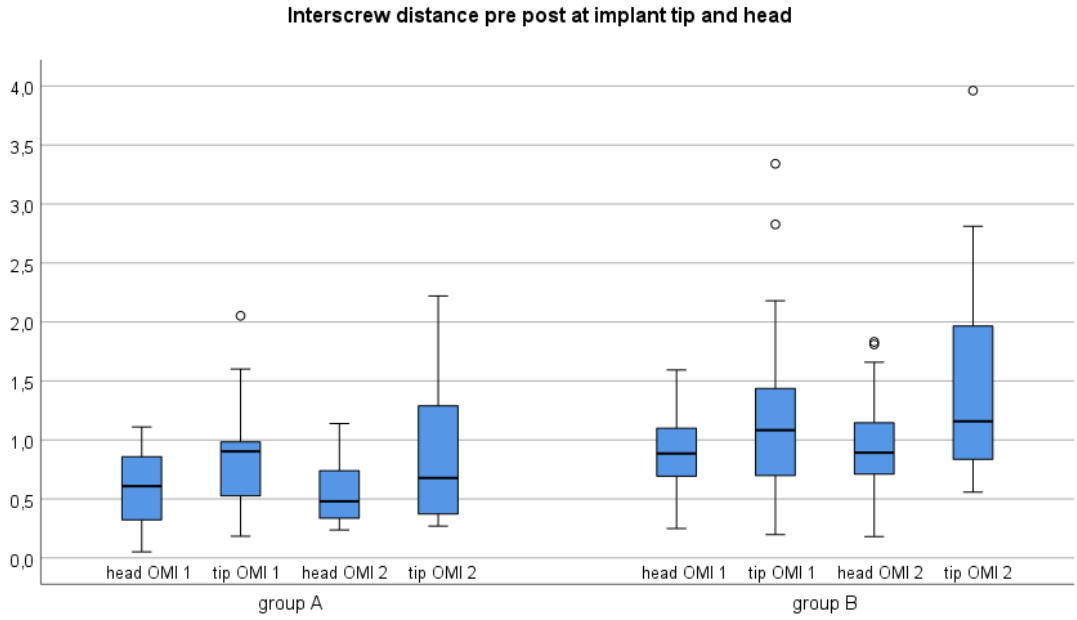

Figure 23: Deviations (mm) between pre- and postoperative coordinates measured at the head and tip of both OMIs in both groups.

[6] Table 5 published as Table 2 in Stursa, L., Wendl, B., Jakse, N., Pichelmayer, M., Weiland, F., Antipova, V. and Kirnbauer, B. Accuracy of palatal orthodontic mini-implants placed using fully digital planned insertion guides: A cadaver study. Journal of Clinical Medicine, 2023.

Displacement of „coronal coordinates“ pre versus post in all 3 dimensions

difference post - pre		Min	Max	Mean	SD	P*
x OMI 1	Group A	-0.50	0.79	0.17	0.39	p = 0.704
	Group B	-0.19	0.71	0.22	0.24	
x OMI 2	Group A	-0.43	0.45	-0.02	0.25	p = 0.947
	Group B	-0.79	0.40	-0.01	0.34	
y OMI 1	Group A	-1.01	0.49	-0.15	0.51	p = 0.002
	Group B	-0.45	1.32	0.61	0.56	
y OMI 2	Group A	-0.93	0.85	-0.18	0.50	p < 0.001
	Group B	-0.10	1.58	0.68	0.45	
z OMI 1	Group A	-0.04	0.89	0.35	0.35	p = 0.051
	Group B	0.04	1.34	0.66	0.38	
z OMI 2	Group A	-0.21	0.85	0.39	0.29	p = 0.043
	Group B	-0.15	1.60	0.73	0.47	

Table 6: Displacement (mm) of coronal coordinates in all 3 planes for both groups measured separately for OMI 1 and OMI 2.

Significant differences in the coronal position of the OMIs were found in the y-axis for both OMIs (OMI 1 $p = 0.002$, OMI $p < 0.001$) and in the z-axis for OMI 2 ($p = 0.043$). The smallest deviations were found for the x-axes, and in total group B presented the highest deviations for y-axis and z-axis.

In both groups the correct insertion depth could not be reached and these findings were significant for both OMIs (OMI 1 $p = 0.02$, OMI2 $p < 0.001$). Insertions were performed too deep in group B (OMI 1: 0.61 ± 0.56 mm; OMI 2: 0.68 ± 0.45 mm) and in group A insertion was not deep enough (OMI 1: -0.15 ± 0.51 mm; OMI 2: -0,18 ± 0.50 mm).

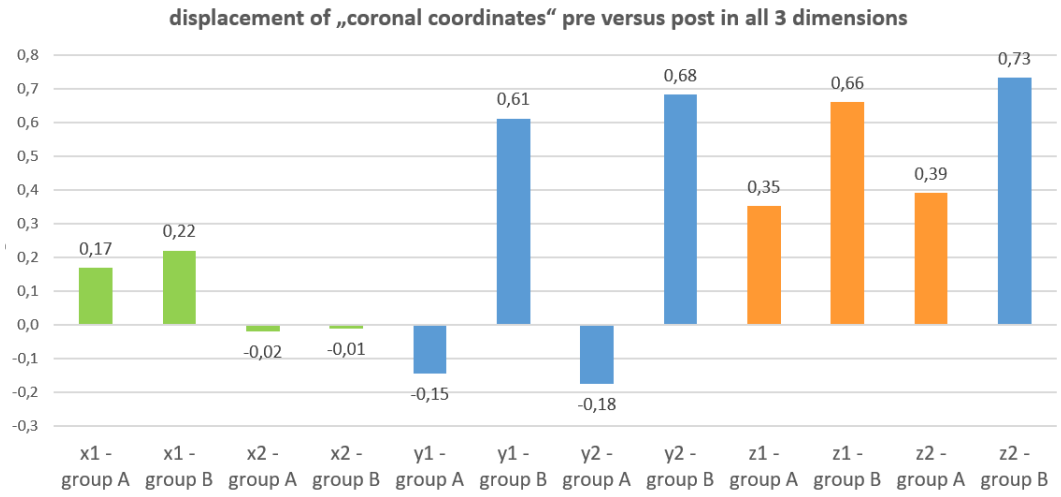

Figure 24: Displacement (mm) of head coordinates measured in all 3 planes.

Displacement of OMI head in relation to raphe-median-plane

As the plane x=0 runs through the raphe-median-plane, positive or negative results indicate the opposite for OMI 1 and OMI 2. A negative result indicates that the post value is smaller than it was preoperatively.

OMI 1: positive result – headpoint post is closer to the center (closer to raphe-median-plane)

OMI 2: negative result – headpoint post is closer to the center (closer to raphe median plane)

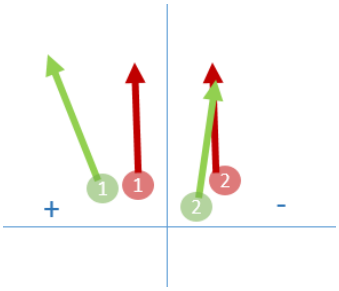

Figure 25: Schematic view of headposition of OMIs in relation to raphe-median-plane.

The mean per direction (center or off center) was calculated as the values have positive and negative signs which would eliminate each other.

	OMI 1				OMI 2			
	center	mean change	off center	mean change	center	mean change	off center	mean change
Group A	8	0.35 (±0.24)	4	0.38 (±0.12)	5	0.21 (±0.18)	7	0.19 (±0.13)
Group B	10	0.28 (±0.20)	2	0.19 (±0.13)	6	0.26 (±0.13)	6	0.28 (±0.26)

Table 7: Displacement (mm) of OMI head in relation to raphe-median-plane, OMI 1 and OMI 2 separately.

In both groups OMI 1 tended to be placed closer to the raphe-median-plane, for OMI 2 the results were quite even in both groups. These findings were not statistically significant.

When OMI 1 and OMI 2 were summed up, in both groups the OMIs had the tendency to be inserted closer to the raphe-median-plane. These findings were not statistically significant.

	both OMIs			
	Center	mean change	off center	mean change
Group A	13	0.30 (±0.22)	11	0.24 (±0.15)
Group B	16	0.27 (±0.18)	8	0.23 (±0.24)

Table 8: Displacement (mm) of OMI head in relation to raphe-median-plane, OMI 1 and OMI 2 separately.

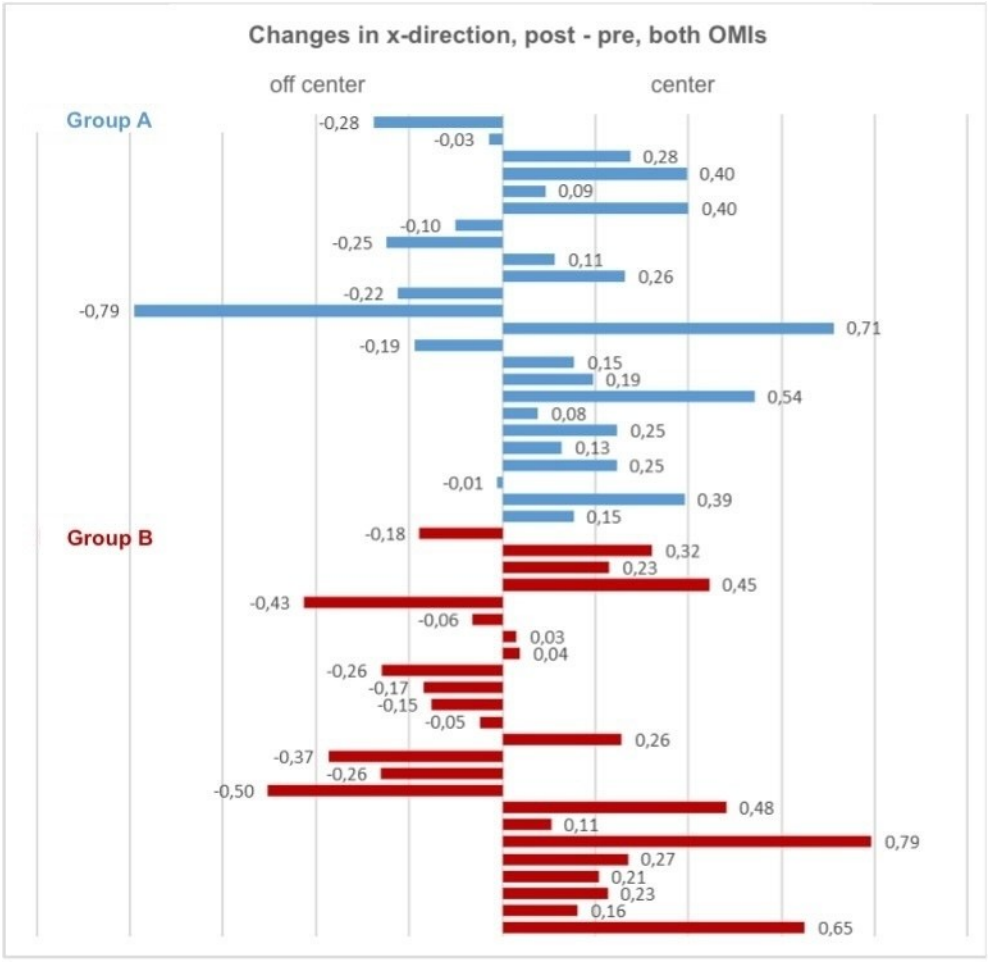

Figure 26: Postoperative changes of head coordinates in x plane (sagittal plane) of both OMIs.

Sagittal and transverse angular deviations

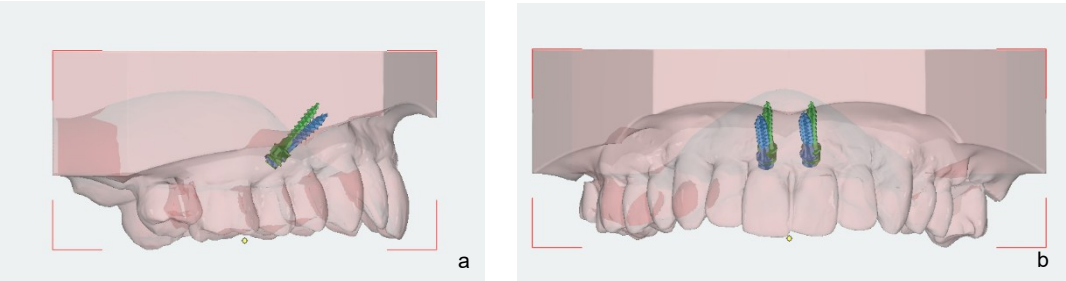

Figure 27: Example of a. sagittal and b. transverse angular deviations (green vs. blue OMIs).

Sagittal and transverse angular deviation, postoperative, angle of axes between OMI 1 & OMI 2

direction		n	Min	Max	Mean	SD	p*
transverse	Group A	12	0.21	13.23	4.81	4.09	p = 0.028
	Group B	12	0.03	27.53	12.66	10.77	
sagittal	Group A	12	0.13	6.42	2.26	1.98	p = 0.929
	Group B	12	0.16	5.10	2.20	1.35	

Table 9: Sagittal and transveres angular deviations (°) between OMI 1 and OMI 2.

A significant (p = 0.028) difference was found for transverse angular deviations between group A and B, with higher deviations in group B (12.66° ± 10.77) compared to group A (4.81°± 4.09). For the deviations in the sagittal plane no significant difference (p = 0.929) was found, as the deviations were quite similar between group A (2.26° ± 1.98) and group B (2.20° ± 1.35).

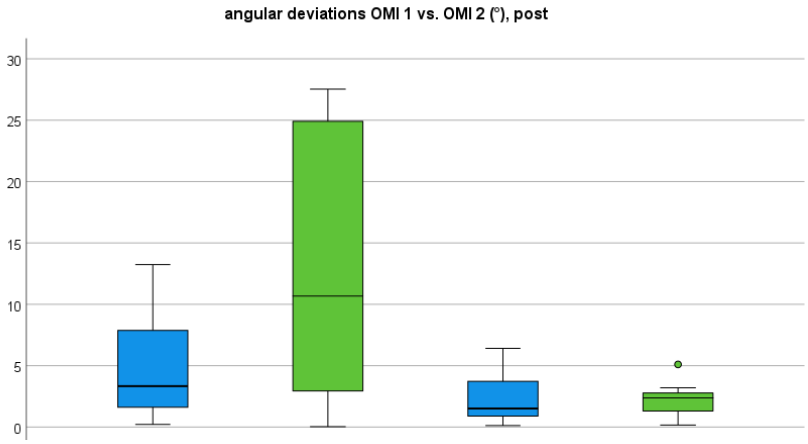

Figure 28: Angular deviations (°) between OMI 1 and OMI 2 in the sagittal and transversal plane.

Sagittal and transverse angular deviations, pre vs post, OMI 1 and OMI 2 separately

plane		OMI	n	Min	Max	Mean	SD	p*
transverse	Group A	1	12	0.46	9.90	4.08	2.63	p = 0.413
	Group B		12	0.01	16.86	5.51	5.35	
	Group A	2	12	0.22	13.48	4.17	4.11	p = 0.157
	Group B		12	0.03	29.33	8.14	8.46	
sagittal	Group A	1	12	0.37	5.34	2.65	1.73	p = 0.527
	Group B		12	0.15	5.80	2.19	1.71	
	Group A	2	12	0.40	15.39	5.89	5.55	p = 0.272
	Group B		12	0.01	29.75	9.21	8.57	

Table 10: Sagittal and transverse angular deviations (°) pre- versus postoperative, OMI 1 and OMI 2 separately.

The sagittal and transverse angular deviations between OMI 1 pre vs post and OMI 2 pre vs post were not statistically significant in both groups. The angles were a little higher in group B compared to group A.

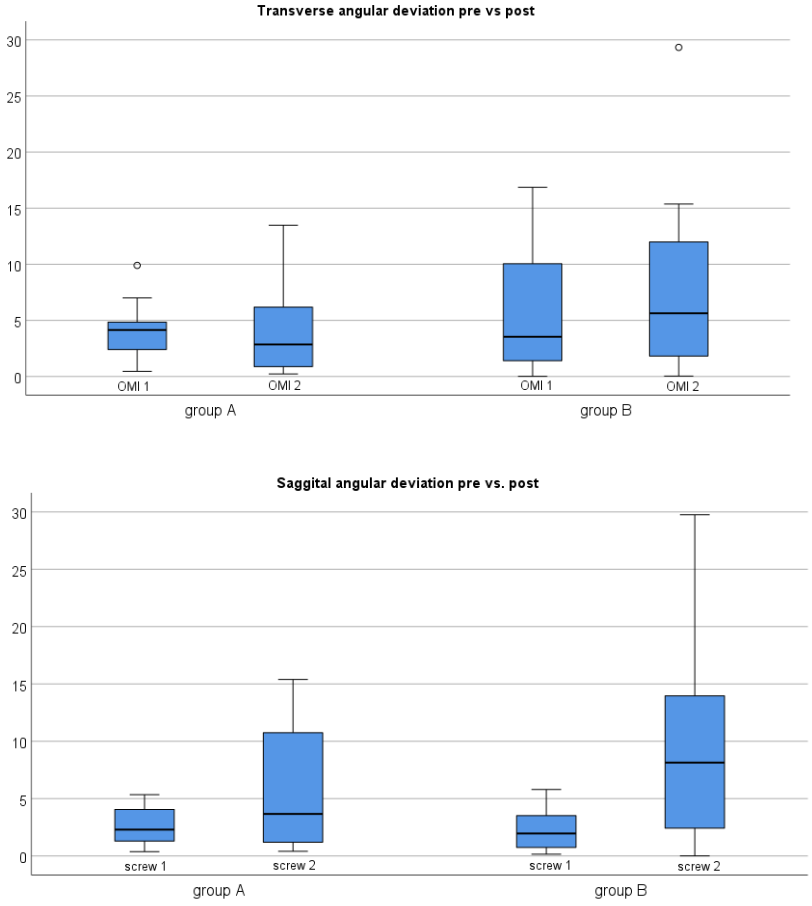

Figure 29: Transverse and sagittal angular deviations (°) pre- versus postoperative, OMI 1 and OMI 2 seperately.

Sagittal and transverse angular deviations, pre vs post, OMI 1 and OMI 2 summed up

direction		n	Min	Max	Mean	SD	p*
transverse	Group A	24	0.22	13.48	4.12	3.37	p = 0.097
	Group B	24	0.01	29.33	6.83	7.05	
sagittal	Group A	24	0.37	15.39	4.27	4.35	p = 0.399
	Group B	24	0.01	29.75	5.70	7.02	

Table 11: Sagittal and transverse angular deviations (°) pre- versus postoperative, OMI 1 and OMI 2 summed up.

The difference between group A and group B for transverse and sagittal angular deviations between pre and postsurgical axes in both OMIs was not statistically significant (p =0.097, p = 0.399). The measured angles were slightly higher in group B in both planes.

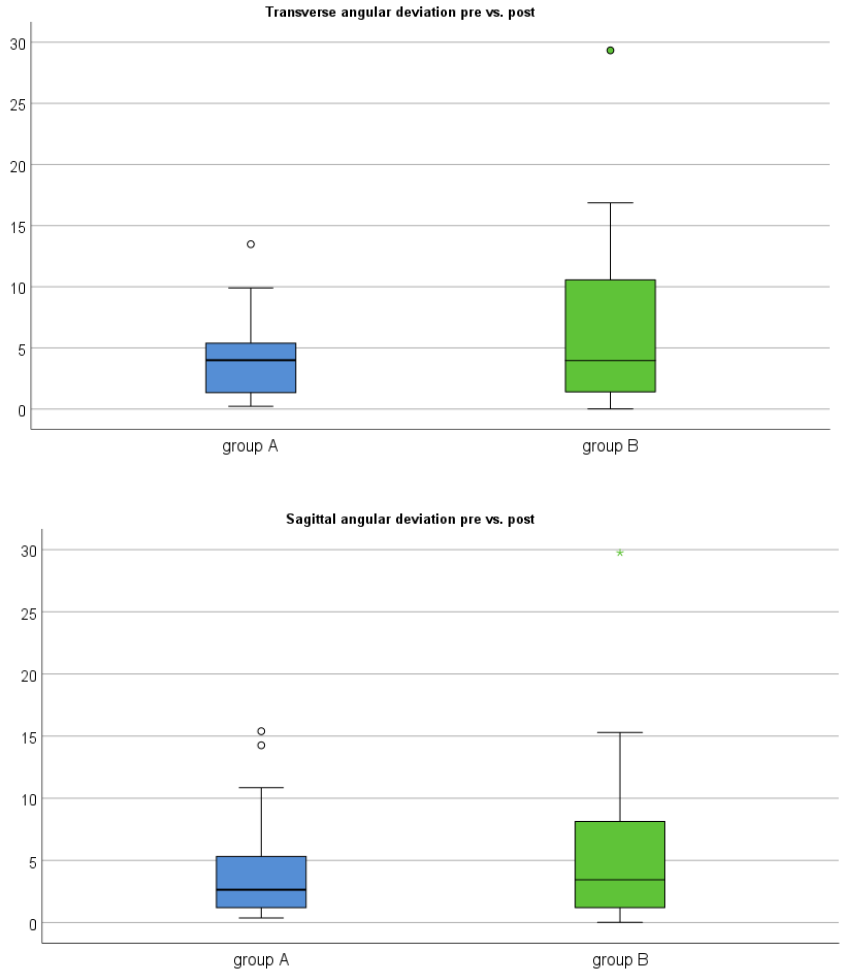

Figure 30: Sagittal and transverse angular deviations (°) pre- versus postoperative, OMI 1 and OMI 2 summed up.

Comparison of all groups

Sagittal and transverse angular deviations, postoperative, angle of axes between OMI 1 & OMI 2

direction		n	Min	Max	Mean	SD	p*
transverse	Group A	12	0.21	13.23	4.81	4.09	p = 0.003
	Group B	12	0.03	27.53	12.66	10.77	
	Group C	8	0.43	8.27	5.02	3.16	
sagittal	Group A	12	0.13	6.42	2.26	1.98	p = 0.007
	Group B	12	0.16	5.10	2.20	1.35	
	Group C	8	0.93	11.50	5.34	0.93	

*Table 12: Sagittal and transverse angular deviations (°) between OMI 1 and OMI 2 in all three groups (*ANOVA).*

The transverse angular deviations were significantly (p=0.003) higher in group B (12.66°± 10.77) compared to group A (4.81°± 4.09) and group C (5.02°± 3.16). A significant statistical difference (p=0.007) was found for sagittal angular deviations in group C (5.34°± 0.93) in comparison to group A (2.26°± 1.98) and group B (2.20°± 1.35).

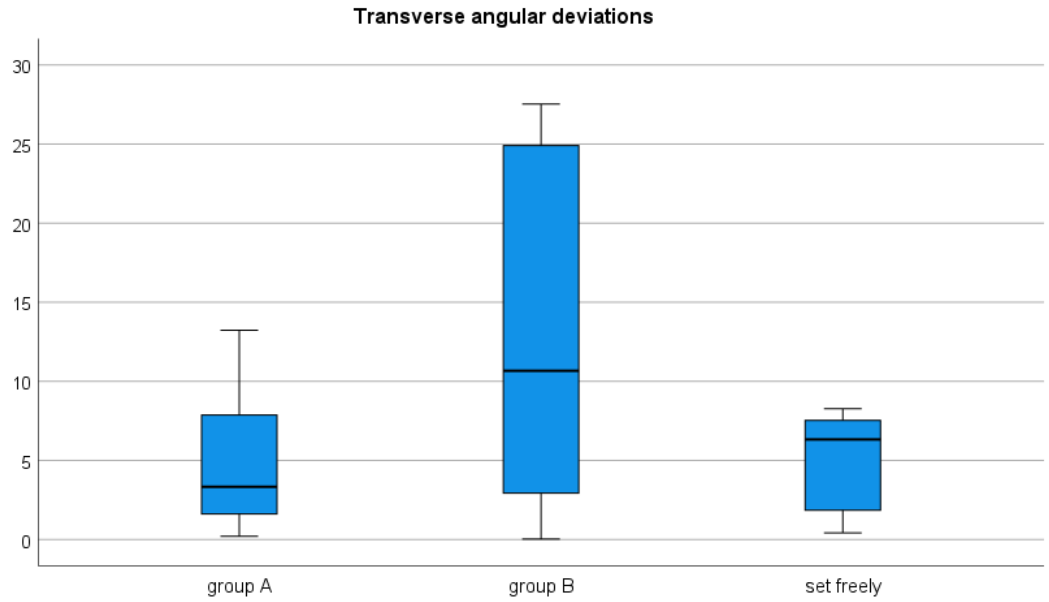

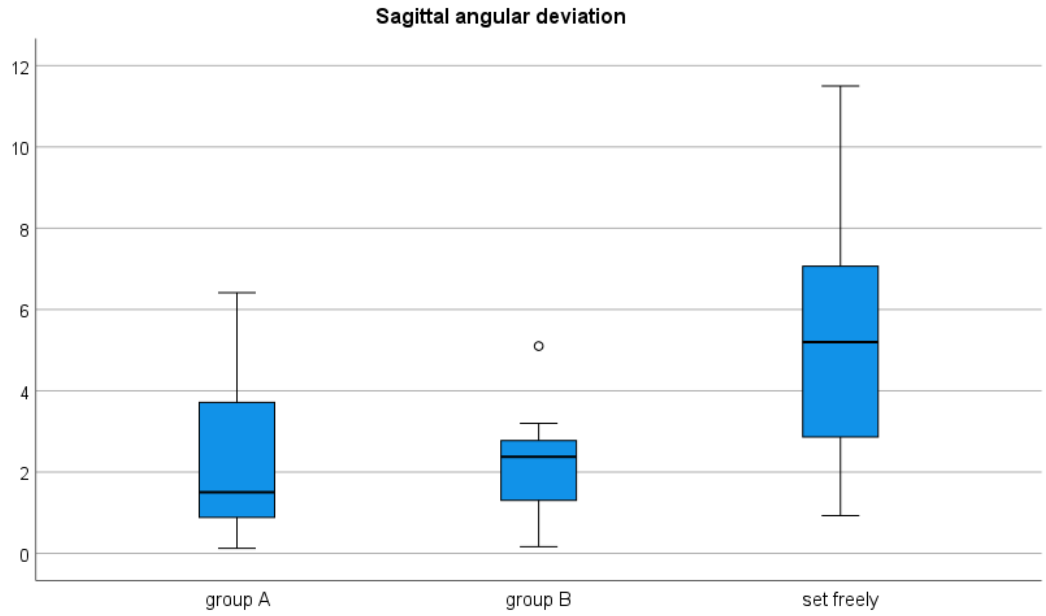

Figure 31: Sagittal and transverse angular deviations (°) between OMI 1 and OMI 2 in all three groups.[7]

[7] Figure 31. published as Figure 5. in Stursa, L., Wendl, B., Jakse, N., Pichelmayer, M., Weiland, F., Antipova, V. and Kirnbauer, B. Accuracy of palatal orthodontic mini-implants placed using fully digital planned insertion guides: A cadaver study. Journal of Clinical Medicine, 2023.

Scanbody results

Comparison of actually achieved positions measured with scanbodies for 6 human cadaver maxillae (H120, H76, G121 – Group A and H152, H30, E154 – Group B) versus CBCT measurements

OMI parallelism of OMI 1 and OMI 2, postoperative CBCT vs. Scanbody measured

	n	Min	Max	Mean	SD	Sign. p*
CBCT	6	0.15	4.35	1.63	1.55	p = 0.831
Scanbody	6	0.12	3.23	1.45	1.19	

*Table 13: Deviation (°) from parallelism between OMI 1 and OMI 2, measured with CBCT and scanbody (*t-test for independent samples).*

No significant difference between both measurement methods (CBCT vs. scanbody) could be detected.

Interscrew distance pre vs. post, Scanbody vs. CBCT

Interscrew distance		n	Min	Max	Mean	SD	Sign. p*
head pre	CBCT	6	6	7	6.83	0.41	
	Scanbody	6	6	7	6.83	0.41	
tip pre	CBCT	6	6	7	6.83	0.41	
	Scanbody	6	6	7	6.83	0.41	
head post	CBCT	6	6.13	7.64	6.91	0.51	p = 0.704
	Scanbody	6	6.31	7.77	7.03	0.49	
tip post	CBCT	6	2.16	7.29	4.58	2.16	p = 0.899
	Scanbody	6	2.38	7.35	4.75	2.2	

*Table 14: Interscrew distance (mm) measured at head and tip level with CBCT and scanbody (*t-test for independent samples).*

No significant difference between both measurement methods (CBCT vs. scanbody) could be found at both measurement levels.

Axial deviation OMI 1 and OMI 2

		n	Min	Max	Mean	SD	Sign. p*
OMI 1	CBCT	6	2.49	13.79	6.44	4.35	p = 0.490
	Scanbody	6	2.31	12.72	6.38	3.83	
OMI 2	CBCT	6	0.83	22.60	9.08	7.50	p = 0.477
	Scanbody	6	1.66	21.55	8.83	6.92	

Table 15: Axial deviations (°) for OMI 1 and OMI 2 measured with CBCT and scanbody.

There was no significant difference between CBCT and Scanbody measurement method found, neither for OMI 1 nor for OMI 2.

Sagittal and transverse angular deviations, postoperative, angle of axes between OMI 1 & OMI 2

		n	Min	Max	Mean	SD	Sign. p*
transverse	CBCT	6	0.92	27.53	15.44	12.83	p = 0.925
	Scanbody	6	0.15	26.35	14.74	12.34	
sagittal	CBCT	6	0.98	4.66	2.27	1.28	p = 0.930
	Scanbody	6	0.24	5.57	2.18	2.04	

*Table 16: Postoperative sagittal and transverse angular deviations (°) measured with CBCT and scanbody (*t-test for independent samples).*

No significant difference between CBCT and Scanbody measurement method was found for transverse and sagittal angular deviations.

Sagittal and transverse angular deviations, pre vs post, OMI 1 and OMI 2 summed up

		n	Min	Max	Mean	SD	Sign. p*
transverse	CBCT	12	0.67	29.33	9.07	8.25	p = 0.463
	Scanbody	12	0.15	28.06	12.79	10.71	
sagittal	CBCT	12	1.64	28.06	8.76	7.68	p = 0.018
	Scanbody	12	0.15	5.57	2.05	1.61	

*Table 17: Sagittal and transverse angular deviations (°) pre- versus postoperatively measured with CBCT and scanbody (*t-test for independent samples).*

The only significant difference was found for sagittal angular deviations, being higher in CBCT measurements (8.76° ± 7.68) compared to the deviations found using scanbodies (2.05° ± 1.61).

Intrarater reliability

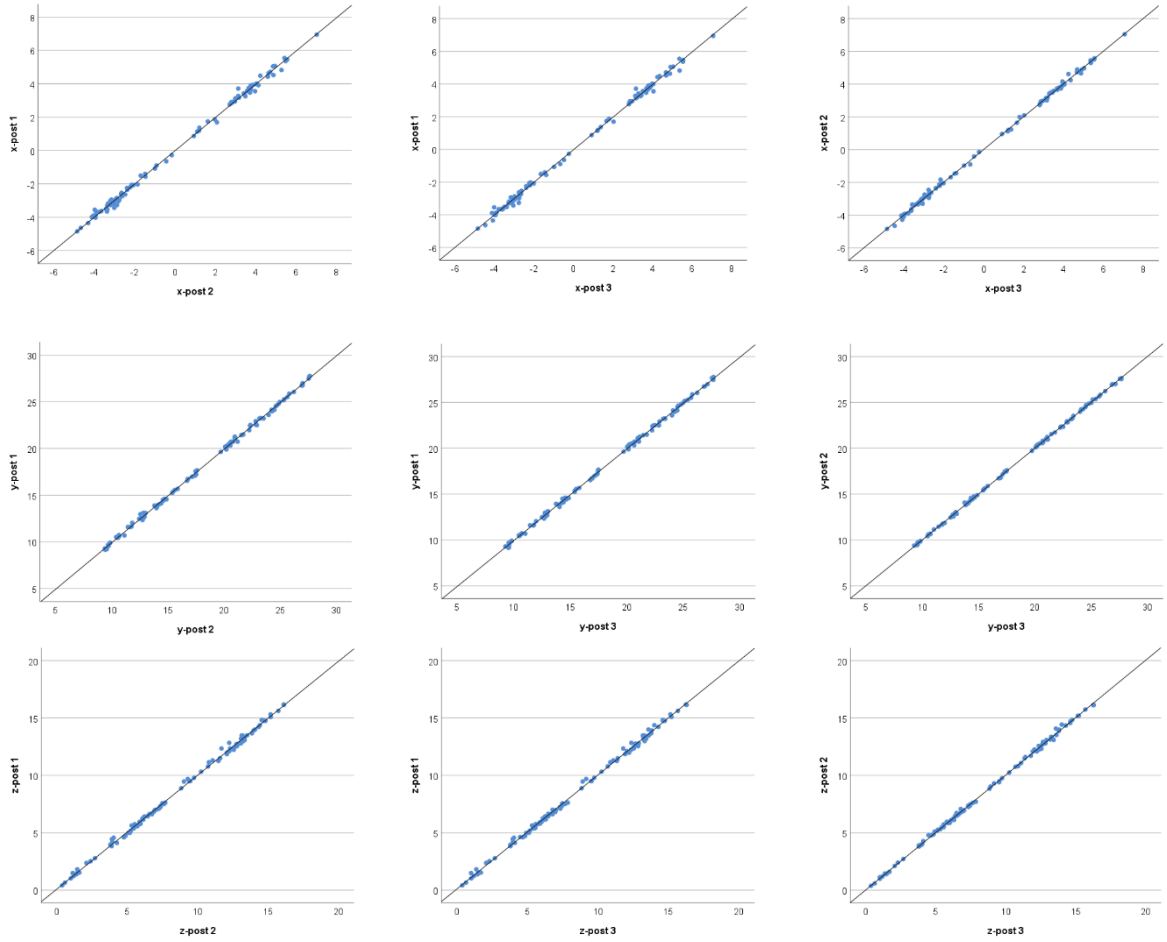

Figure 32: Intrarater reliability.

All measurements were repeated three times for each coordinate. The ICC (intraclass correlation coefficient) was found to be 0.999.

Discussion

In this study we evaluated the levels of accuracy and reliability of the transfer of a virtual planning process with two different kinds of surgical templates, looking at sagittal and transverse angular deviations between planned and actual positions and OMI parallelism was assessed. The accuracy assessment was done by superimposition of virtual planning models and postsurgical CBCT scans. Statistically significant differences were found for all methods, although group A presented superior results compared to groups B and C.

A further aim of the study was the comparison of guided OMI insertion with conventional freehand insertion. Insertion in Group A was superior to Group C regarding sagittal and transverse angular deviations, whereas the guides of group B proved to be less accurate for transverse angular deviations. Hence it became evident that neither freehand nor guided OMI insertion could achieve the intended position with 100% accuracy. The proposed hypothesis, that there is no difference in transfer accuracy between the investigated insertion guides, was thus rejected.

Prior research has investigated different insertion guides, concluding that their application enhances the accuracy and stability of OMI insertion while diminishing the failure rate of mini-implants (84, 92, 96, 120, 121, 122, 123). Tooth-supported guides, supported on the edges of teeth and rigidly printed, were found to provide higher insertion accuracy compared to templates supported solely by the gingiva (84, 98, 124). Given these findings, we decided to examine only tooth-supported, 3D printed surgical guides in our study. According to Baumgaertel et al. (125) dental measurements made on CBCTs are precise and reliable, hence we decided to perform postsurgical accuracy measurements using CBCTs. We performed the measurements following the method outlined by Cassetta et al. (91), which involves the comparison of pre-and postsurgical CBCTs to calculate angular, coronal and apical deviations between digitally planned and actual TAD positions.

In the present study all actual screw positions, delivered by a surgical guide, differ from the digitally planned screw positions in all planes in both groups (Group A and B). The insertion technique using the surgical guide of Group A exhibited consistently lower deviations between planned and actual positions in all examinations than in Group B, although not all results were statistically significant. The only exception is the sagittal angular deviation for OMI 1 in Group B, which was on average 0.46° smaller than in Group A.

The insertion using the drilling template of Group A was subjectively perceived as easier, as its fit seemed superior and there was no sensation of the template lifting off, as was noticed in some cases using the surgical template of Group B. An assistant holding the insertion guide in position during insertion appears to be helpful, regardless of the type of surgical guide.

All OMIs exhibited parallelism between left and right OMIs preoperatively, but postoperatively none of the inserted miniscrew pairs proved parallelism. The amount of deviation between left and right OMI were assessed with the angles between both implant axes and were significantly (p = 0.03) smaller in group A (5.19° ± 2.71°) than in group B (10.41° ± 7.29°). The investigation for parallelism could not reveal statistically significant differences between the left and right mini-implants in either group. According to Migliorati et al. (126) OMIs do not remain absolutely stable under orthodontic loading and undergo angular displacements up to 11°. Hence, it is evident that even initially parallel pairs of mini-implants do not remain parallel to each other throughout the entire treatment. Ludwig et al. (53) reported an angle of the implants to one another of 5.28° for non-sterile and 2.99° for sterile insertion guides, hence achieving 100% parallelism with their insertion guides was not possible either.

The vertical inaccuracies observed in our study align with the findings of Kniha et al. (124) and Möhlhenrich et al. (84), who attributed the vertical disagreement between planned and actual OMI positions to drill sleeves that did not reach the final position on mini-implant pillars in the guide fabrication process or to the resilient properties of silicone. Kniha et al. (124) found that the radiological evaluation of vertical deviations revealed significantly higher transfer accuracy levels compared with intraoral scan evaluations of the same study population. They were able to demonstrate that solely gingiva-supported guides allow for lower insertion precision compared with tooth-supported guides, that were rigidly printed and supported on the edges of teeth (124). Based on these findings, we decided to investigate only tooth-supported guides. Ludwig et al. (53) reported lower vertical discrepancies, however, their study was conducted on bone substitute blocks and the surgical guides were attached to the boneblock using auxiliary screws. The deviation in insertion depth observed in our study may be related to the different levels of rigidity of the surgical guides of Group A and Group B. The in-house fabricated templates in Group B have been less rigid, resulting in deeper insertion, whereas the commercially available guides were more rigid, making it impossible to reach the final insertion depth. The fit of Group A's insertion guide appeared to be superior, most likely due to their more pronounced extension to the buccal tooth surface compared with Group B, whereas the in-house-fabricated guides sometimes appeared to lack reliable stability and did not stay in place without the assistance of fixation. Different printing configurations and offsets

between the two groups may also be factors contributing to these variations. Appropriately designed insertion guides include a built-in depth stop, enabling accurate attainment of the insertion depth (55). This guarantees adequate penetration in the bone, while at the same time it prevents a too deep insertion (55).

The mean interscrew distance between left and right OMI decreased in both investigated groups, both at the level of the implant head and at the level of the implant tip. This finding could also be attributed to the varying levels of rigidity of the drill templates and the resulting loosening of the guides during insertion. Additionally, the miniscrews are inserted into dense bone, without predrilling, which initially causes resistance and may result in detachment of the insertion template. Hence, predrilling seems advisable even with self-drilling screws because the increased insertion pressure can make it difficult for the clinician to maintain the correct insertion direction (2).

An accurate interscrew distance at the head level is important, particularly when prefabricated corresponding orthodontic appliances are to be inserted within the same session. If the deviation from the digitally planned target position is too significant, it may result in the device not fitting properly, necessitating adjustments from the laboratory. According to Ludwig et al. (53) their mean deviation to the planned implant head positions of 0.81% is clinically acceptable and reproducible by using CAD/CAM surgical guides. Further studies defining clear tolerance levels for simultaneous insertion of TADs and the corresponding appliance are needed.

Deviations between planned and actual OMI coordinates measured at the head and the tip of both OMIs showed significant differences between Group A and Group B. Mean deviations at the level of the OMI head in Group A were 0.60 mm for OMI 1 and 0.56 mm for OMI 2, whereas in Group B the mean deviation measured for OMI 1 was 0.90 mm and for OMI 2 0.96 mm. The deviations at the tip were even higher, with 0.87 mm for OMI 1 and 0.87 mm for OMI 2 in Group A and in Group B 1.17 mm for OMI1 and 1.43 mm in Group B. This phenomenon of higher deviations at the level of the implant tip aligns with the study of Mang de la Rosa et al. (98). Kniha et al. (124) reported deviations at the implant tip of 1.77 mm and at the implant shoulder of 1.47 mm, which indicates slightly higher deviations than revealed in our study. Deviations at the level of the implant tip are no less important, as these discrepancies could lead to injury of adjacent anatomical structures. Errors arising at the beginning of the insertion process lead to increased inaccuracy at the level of the implant tip (98), hence, to reduce the risk of anatomical injuries a safety distance regarding the implant length is pivotal (84).

In both groups the actual OMI positions tended to be closer to the midpalatal suture than in the virtual target positions. An approach to diminish the potential risk of trauma in the area of the median palatine suture in growing patients, would be a slightly increased interscrew distance, as according to Asscherickx et al. (50) we cannot certainly exclude the possibility that insertions into the palatal suture may affect normal transversal growth.

No significant angular deviations between planned and actual screw positions were found for right and left OMIs in both groups, however, the deviations were larger in Group B. Even when both groups were combined, no significant difference between left and right mini-implants was observed. The mean angular deviations were 4.90° for OMI 1 and 5.36° for OMI 2. This finding aligns with the results of Iodice et al. (127), who also found no significant difference between right and left OMIs and concluded that the operators position at the chair has no influence on mini-implant positioning. Like in their study (127), all our implants were placed by a right-handed operator. Casetta et al. (91) reported mean angular deviations of 4.60°, which is quite similar to our findings. Another study using postoperative CBCTs found angular deviations of 2.81° (124).

Möhlhenrich et al. (84) performed postsurgical intraoral scans with scanbodies for accuracy measurements and found sagittal angular deviations of 3.67° and transverse angular deviations of 3.60°. Our study showed higher transverse angular deviations with 4.81° in Group A and 12.66° in Group B, but sagittal angular deviations were smaller with 2.26° in Group A and 2.20° in Group B.

The present study also compared the two surgical guides with conventional freehand insertion. In doing so, Group C exhibited the highest inaccuracy for the sagittal angular deviation between the two screws. The mean deviation for the freehand group was 5.34° and in the accuguide group a mean deviation of 2.26° was found and in the selfdesigned guide group inaccuracies of 2.20° were detected. In Contrast, Group B exhibited the highest inaccuracy for the transverse angular deviation at 12.66°. Group A had the lowest deviation at 4.81°, with Group C showing slightly higher deviations at 5.02°, only minimally larger. To best of our knowledge no study has yet examined the difference in accuracy between surgical guides and freehand insertion, but Nienkemper et al. (55) compared the success rates of guided and conventional insertion and found no significant difference. The success rate for guided insertion was 97.37% and for freehand insertion it was 97.69% (55).

In modern dentistry, 3D imaging has become indispensable across all dental specialties (128). Alongside the widespread adoption of CBCT imaging and its ability to apply extremely low radiation doses in recent years, multiple digital tools for treatment planning and analysis were introduced (112). Intraoral surface scans allow for the generation of accurate surface models of teeth and gums (112), thus intraoral scans have widely replaced conventional impressions due to their superior precision (129). The availability of digital impressions and the options of image fusion algorithms have opened the way for numerous digital workflows, and scientific research has pointed out that these digital workflows are at least as precise and effective as traditional methods (112).

CBCT scans have become key diagnostic tools, particularly in surgical dentistry, due to their ability to precisely depict the 3D shape and position of the teeth and jaw bones (130). Compared to traditional CT scans CBCT enables quicker data acquisition and comes with advanced software tools for image processing and measurements (125). Because of the low radiation dose and the outstanding spatial resolution of CBCTs, they are gaining popularity as a useful tool for diagnosis and treatment planning (112).
Lateral cephalograms, traditionally used in orthodontic practice, are limited due to their two-dimensional nature, leading to image distortion and overlapping of bilateral structures, as they are projections of three-dimensional anatomical structures (131). According to the as low as reasonably achievable (ALARA) principle, all diagnostic questions should be approached by exposing the patient to the lowest feasible radiation dose, based on medically justified indications (132).
Jung et al. (132) showed in their study that lateral cephalometric x-rays provide a reliable assessment of vertical bone quantity for paramedian OMI insertion. Palatal vertical bone dimensions of 18 cadaver skulls were examined on lateral cephalograms and CBCTs (132). They compared the quantity of bone height analyzed on CBCTs with measurements made on lateral x-rays (132). A notably higher palatal bone height was found on CBCTs and following the authors concluded that the use of lateral x-rays for planning of paramedian TAD insertions is appropriate (132). Lateral cephalograms often underestimate the available vertical bone quantity, expressing a minimum bone quantity, hence the use of CBCT may be limited to select cases with marginal bone amount (132). This assumption was emphasized by Kim et al. (113) who found that the palatal bone at 5 mm off-center was likely to be shown as palatal bone contours and bone at 1.5 mm was found to be thicker than displayed on lateral cephalograms.
In the present study, 3D imaging was used to measure accuracy and to investigate interferences with neighboring anatomical structures. Nonetheless, in clinical practice, an approach like that proposed by Maino et al. (87), combining lateral cephalograms and digital

dental models for surgical template planning and production, might be sufficient. The substitution of CBCTs with a lateral cephalometric x-ray for virtually planning of paramedian OMIs comes with a decrease in radiation exposure for the patient (55). Since lateral cephalograms are routinely taken during case planning, there is no requirement for an additional x-ray for the implant planning process (55). In patients with displaced teeth, limited bone supply or other pathologies, including clefts, 3D radiographs can be particularly beneficial in identifying optimal insertion sites and angles for OMI positioning and the fabrication of insertion guides (92).

Von See et al. (133) presented a method to assess the 3D position of dental implants after insertion in a radiation-free manner, without the need of reuse of x-rays. For this technique scanbodies are placed on the implants, subsequently intraoral scans are obtained and merged with a three-dimensional dataset (133). This nonradiological technique was found to be a precise tool for the assessment of implant positions and enables the determination of deviations between planned and actual implant positions (134). Möhlhenrich et al. (84) adopted a comparable approach for accuracy assessment of orthodontic mini-implants inserted using surgical guides. They fixed corresponding scanbodies on the OMIs and performed intraoral scans which were superimposed with the planning model via the pillars used as reference (84). These measurements focused on deviations in the oral aspect of the mini-implant, essential for installing an orthodontic device (124). Nevertheless, the intra-bony precision is also of interest due to the potential risk of trauma to neighboring anatomical structures (124). In a study comparing postoperative scanbody and CBCT accuracy measurements, significant differences between the two methods were found (124). It was shown that there is higher agreement between virtual planning and direct measurement in the CBCT scans, outlining a higher transfer accuracy than previously assumed from intraoral scan results (124). In our study, we also applied scanbody measurements, although with a smaller sample size (n=6) since this testing was performed at a later stage. There was occasionally a sense that the OMI position might have been changed during scanbody attachment and removal, which could be a consequence to the fact that OMI insertions were performed a while ago and they were inserted in human cadaver maxillae. The results should therefore and especially due to the small sample size, be interpreted with caution.

A fully digital workflow, involving intraoral scanning, digital planning and subsequent 3D printing, allows for CAD/CAM fabrication of orthodontic devices (118). This method comes with several advantages, including a faster workflow, since models are instantly available to the orthodontist without the need of a dental laboratory (118). Additionally, certain downsides

associated with conventional impressions, such as gag reflex, patient discomfort and storage of impression material can be avoided (118). The whole digital workflow, beginning with virtual OMI insertion planning to appliance design, was introduced to the orthodontic world some years ago (135). Owing to the possibility of simultaneous digital manufacturing of the surgical guide and the corresponding orthodontic appliance facilitates a single-visit protocol for the placement of mini-implants and superstructure (135). In the event of appliance loss or breakage, no new impression is required, as a copy from the digital archive is immediately available (118). Thanks to the fully digital workflow the communication between orthodontist and laboratory technician becomes easier and more predictable devices are available, resulting in improved treatment options for the patient (118). However, in a one-visit workflow, the main focus should lie on accurate mini-implant insertion, as even minor axial deviations can prohibit the insertion of the corresponding appliance (135). Hence, the success of a single-visit protocol depends on a precise OMI placement, especially when multiple TADs and a rigid orthodontic appliance are required (136). With an increasing number of mini-implants used and more complex and rigid corresponding devices, the tolerance threshold for inaccuracies lowers (136). If a certain tolerance level is exceeded, resulting in misfit of the device, then a two-step protocol, requiring a new digital impression, must be implemented (136, 137). Clinically, the most important factor for a good appliance fit is the coronal distance, but other parameters such as the insertion depth, the angle of two OMIs to one another and the angle of the OMI to the surface should also be kept in mind (53). Another important point is the direction of the deviation, meaning that in unfavorable cases the deviations are divergent, but in a few favorable cases these deviations can compensate for each other (136). These deviations can occur at the implant tip as well as at the level of the OMI head and all positions in-between (136). The study of Pozzan et al. (136) found that a certain amount of deviation was inserted at each step of the workflow and the laboratory step was found to have significantly smaller impact on the deviation than the clinical step. The cause of this raised susceptibility to deviations may be related to the clinician, depending on his experience, as well as to the patient, with factors such as bone density and quality (136). According to a systematic review, that evaluated the precision of surgical guides used in dental implantology, clinically acceptable deviations were found with results showing mean angular deviations of 3.5° and average vertical deviations of 1.2 mm and 1.4 mm at the implant head and tip (138).

The anterior palate has emerged as the favored region for OMI placement, particularly due to its ample bone supply and the omission of dental roots (98). Despite their establishment in orthodontic clinical practice mini-implant insertion can come with risks if the clinician is lacking profound knowledge about the anatomy of the insertion site (87). A main advantage of palatal

insertion is the fact that the miniscrews are not interfering with any teeth as they are not in the path of movement (139). As the anterior palate offers thin attached gingiva and good bone quality, high success rates are ensured (139). Even though this region is deemed as a safe zone because of the absence of dental roots, the palatal thickness is not coherent, hence analysis of bone availability for OMI placement is crucial to ensure primary stability and reliable anchorage (87). The “T-Zone”, known as the region immediately behind the third palatal rugae, is a safe and appropriate insertion area for mini-implant placement (44). OMI placement is typically a soft tissue flapless surgical procedure, mostly relying on prior studies outlining average bone height and well-defined “safe zones” (96). To date most clinicians are still performing freehand mini-implant insertion, but the use of surgical guides is increasing in popularity (55). Hourfar et al. (140) claimed that a safe freehand insertion of TADs in the anterior palate is possible with the assistance of certain anatomical guidelines. In the planning of an OMI-supported orthodontic device, at least two appointments are required as it is impossible to predefine the exact TAD positions beforehand, even though freehand insertion is typically considered as safe and precise (44). Nienkemper et al. (55) have shown that conventional insertion is able to obtain similar levels of success compared with guided insertion. Our study demonstrates that, when both workflows are compared, similar interscrew parallelism can be achieved with and without the use of surgical guides. It should be noted that both in our study and the study by Nienkemper et al. (55) TAD insertions were performed by highly experienced specialists. Although the abovementioned clinical landmarks have been well studied and often published, many clinicians are hesitant in using OMIs as they are not immediately acquainted with the placement procedure (127). This phenomenon was supported with the findings of an international survey, indicating that most orthodontists use OMIs rarely or sporadically (141). A significant difference between specialist training in the clinic under supervision and orthodontists in private practices was found, with 56% using OMIs in a university setting versus 15% in a private clinic (141). The use of an insertion template could help clinicians overcome their inhibitions (127). However, a successful digital workflow includes a steep learning curve and relies on the doctors’ skills and experience (101). Another requirement for the implementation of the CAD/CAM process are specialized software solutions and it is possible to outsource either the planning, the manufacturing or both to external service providers (e.g. accuguide by Forestadent) (110).

The comparison of our study with others is challenging owing to the variability of reference points and measurement techniques across the published studies. Differences in anatomical regions, study protocols and measurement methods hinder direct comparisons (84, 92, 124, 127, 136).

In 2016 Maino et al. (87) published a descriptive article showing the design and use of an insertion guide, called “MAPA System”, for palatal mini-implant insertion. They identified the ideal insertion region using a cephalometric x-ray, requiring a thermoplastic bite registration with radiopaque markers along the median palatine raphe, or a CBCT and superimposed a digital model onto it (87). For the data fusion and the virtual design of a surgical guide they used the software “eXam Vision” and “Rhinoceros” (87). For replication of the insertion angle and prevention from too deep penetration two cylindrical guides are designed and seamlessly connected to the template by transparent resin bridges (87). The tooth supported surgical guide is 3D printed and requires removal of the bridges once the OMIs are inserted (87). With two case reports they underlined the success of the applied technique (87). The group did pioneer work in showing that for palatal OMI position planning one can abstain from 3D radiographs and their approach of using radiopaque markers seems to allow for accurate superimposition (87). However, a drawback is the removal of the surgical guide, requiring separation of the cylinders from the template using a dental bur (87). No accuracy measurements were performed (87), but the article served as guideline for digital planning in subsequent publications (84).

Cassetta et al. (91) investigated the accuracy of 3D printed insertion guides in five patients using pre- and postoperative CBCTs. For virtual planning, digital models and CBCT datasets, where patients wore radiological trays with radiopaque landmarks, were merged using dedicated software (Vector 3D) (91). The ideal insertion sites for the OMIs were determined and subsequently a tooth supported surgical template was virtually created and 3D printed (91). Special cylinders were used to accommodate drill handles and serving as depth stops (91). Postoperatively a CBCT was performed in all patients and another dedicated software (Mimics software) was used to superimpose the pre- and postoperative CBCT datasets (91). The 3D coordinates of the OMIs at apical and coronal level were used for deviation measurements (91). The mean coronal and apical deviations were 1.38 ± 0.65 mm and 1.73 ± 1.03 mm, while the mean angular deviation was found to be 4.60 ± 2.54° (91). The mean axial deviations found for both surgical guides in our study are quite similar to these findings, while the apical and coronal differences were slightly smaller in our study. The chosen sample size in this study was very small, however it was conducted in a clinical setting rather than on models or human cadaver heads.

In 2020 Möhlhenrich et al. (84) performed a human cadaver study, investigating the transfer accuracy of 10 gingiva borne (GBG) and 10 tooth borne (TBG) surgical guides. Plaster models were converted into digital models and merged with lateral cephalograms using TADmatch

module (OnyxCeph) (84). After TAD position planning, working models with pillars for receiving parallel drill sleeves were 3D printed (84). Metal drill sleeves were placed on mini-implant pillars and were gripped with two component silicone to receive the surgical guides (84). For accuracy measurements scanbodies were applied on the OMIs and an intraoral scan was performed (84). The planning model and the scanbody model were aligned using an ICP algorithm with software support (Geomagic) and accuracy measurements were performed (84). Statistically significant differences were found for lateral deviations between TBG and GBG, with 0.88 ± 0.46 mm for TBG and 1.65 ± 1.03 mm for GBG (84). The results of the tooth borne guides are in line with our findings for coronal deviations. Another significant finding were sagittal angular deviations of 3.67 ± 2.25° for TBG versus 6.46 ± 5.5° for GBG. Vertical deviations of 2.34 mm versus 2.14 mm and transverse angular deviations of 3.60° and 4.06° presented no significant difference between the two insertion guides. The reduced radiation exposure through the use of lateral cephalometric x-rays for position planning and the radiation-free accuracy evaluation method using scanbodies is beneficial. However, this does not offer information regarding the mini-implant tip, which could potentially result in measurement inaccuracies and may not be disregarded for anatomical reasons. It seems that the quality of body donors is superior to our sample as they used non-fixed fresh heads of body donors and our sample consisted of body donor heads fixed with a modified-Thiel technique.

Kniha et al. (124) performed an extension of Möhlhenrich et al.'s (84) study and obtained postoperative CBCT scans of the same study sample. They performed accuracy measurements on superimpositions of planning model and postoperative CBCTs in CoDiagnostiX and compared it with the scanbody results (124). They found statistically significant differences between TBG and GBG regarding implant angulations, with more precise findings for TGBs (124). No significant differences could be observed for measurement accuracy of angular deviations for TBGs and GBGs between oral scans and CBCTs (124). Higher lateral deviations were found on CBCTs for TBGs than on intraoral scans, while vertical deviations were lower measured on CBCTs compared to intraoral scans (124).

Ludwig et al. (53) examined 60 identical insertion guides used on bone substitute blocks, with 30 guides being sterilized and 30 guides being left non-sterilized. The 3D printed resin insertion guides were fixed at solid-rigid-foam bone substitute blocks for the insertion process and after insertion a steel strip was attached between drill template and bone blocks for a radiopaque layer for postoperative CBCTs (53). Postoperative accuracy measurement was performed using OnyxCeph software and each mini-implant received two measurement points, one at the implant tip and one at the implant head (53). For the sterilized guide group they found mean

coronal deviations of 0.057 mm and apical deviations of 0.428 mm as well as mean vertical inaccuracies ranging from 0.073 – 0.15 mm (53). Surgical guide precision could be enhanced due to heat treatment during the sterilization process (53). Our study investigated non-sterile surgical templates. Future studies should investigate sterilized drill templates, also in ex-vivo examinations, to increase transfer accuracy, as postulated by Ludwig et al. (53). To date this study presented the highest accuracy outcomes for 3D printed surgical guides.

Migliorati et al. (95) performed a study to investigate the accuracy of surgical guides in twenty-five orthodontic patients. For the digital planning procedure, an intraoral scan and a lateral cephalogram were superimposed, and subsequently they placed the mini-implants virtually using the OnyxCeph software (95). Laboratory models with holes corresponding to the OMI positions, in which laboratory analogues were positioned, were 3D printed (95). Subsequently thermoformed sheets were used and cropped in the OMI area, before mini-implant analogues were placed and metal sleeves were fixed on the analogues head together with the drill blade (95). The last step was fixing the metal sleeves and the thermoformed part by using resin (95). After insertion they used scanbodies for postsurgical accuracy evaluation, and they also performed the scanbody procedure on the laboratory analogues, which served as a control group (95). The highest deviations were observed between the achieved and planned positions, with median differences of 6.22° (95). There were also vertical inaccuracies as the inserted OMIs were not as deep as planned (0.76-1.16 mm) (95). Appliance installation worked without problems, hence the deviations cannot be deemed clinically significant (95). A cause of lateral and vertical inaccuracies in scanbody measurements could be compression occurring between the scanbody base and the palatal soft tissue during the intraoral scanning process (95).

A systematic review claimed that most published papers investigating surgical guides include too few cases and lack suitable control groups to effectively evaluate the potential benefits (123). They attribute the publication bias and the diversity to the continuous technological advancements in dentistry (123). Even though they report a low methodological level amongst the studies, they conclude that the application of surgical guides improves mini-implant accuracy and stability and can reduce the failure rate of OMIs (123).

Despite promising results, this study is subject to limitations. First, there is a difference in age between the body donors, who are mostly of advanced age presenting different dental issues such as missing or filled teeth, dental implants or prostheses, and the common orthodontic clientele, who are mainly adolescents with complete dentition (142). With an increase in age

comes a regression in bone height at the palatal process of the maxilla, which is also clinically relevant when choosing the appropriate implant length (143). Thus, the chosen study population does not ideally represent typical orthodontic patients.
Second, the choice of embalmed specimen with preserved tissue does not allow for an authentic representation of the clinical scenario, due to the absence of blood perfusion (124), changed tissue quality and properties following preservation, and the lacking bone remodeling (144).
Third, artifacts originating from prosthetic restorations in the cadavers' CBCT datasets might have impacted the accuracy of superimposition. In case of existing artifacts, the localization and identification of the reference points or areas to be superimposed have proven to be difficult (130). CBCT artifacts, provoked by metal attachments, like orthodontic brackets or prosthetic crown restorations, have an impact on the integration performance (130).
Another limitation of the study is the chosen sample size, as ideally, n=12 would have been suitable for all three investigation groups. Nonetheless, as a lack of appropriate body donors was available during the study period, we settled for n=8 for Group C, looking at it as an additional group alongside the main investigation groups A and B.
A further limiting factor of this study could be the omission of pilot drilling. Even tough dispensable for self-drilling OMIs, as used here, the initial resistance of the cortical bone may require an increased insertion pressure, making it hard to keep the correct insertion direction or potentially resulting in detachment of the surgical guide (2).
Finally, the behavior of hard and soft tissues in the body donors may vary from that found in a real clinical setting.

So far, there are few studies examining the transfer accuracy of guided mini-implant insertion using postoperative CBCTs. To our knowledge, only two such studies have been performed in a clinical setting. Cassetta et al. (91) compared pre- and postsurgical CBCTs of five orthodontic patients receiving palatal OMIs, while Liu et al. (93) examined surgical guides for interradicular TAD insertion using postoperative CT scans. Bae et al. (92) used insertion guides for interradicular OMI placement in twelve cadaver maxillae and examined the transfer accuracy using pre- and postsurgical CBCTs. Kniha et al. (124) performed another body donor study using presurgical lateral cephalograms and postoperative CBCTs. In line with previous studies aimed at avoiding possible sequelae of radiation exposure to living subjects, the present study stuck to this approach by limiting the analysis to embalmed specimens. In a next step a clinical study investigating the accuracy of surgical guides, preferably including alternative imaging techniques with minimized radiation exposure, should be carried out. Considering that scanbody measurements focus only on the oral part, possibly incomplete data regarding the

orientation of the implant tip may be delivered, which is why CBCT based investigations are clinically relevant. It is pivotal that precise visualization of the implant tip is ensured in clinical settings to impede damage to adjacent anatomical structures.

While numerous studies have analyzed the accuracy of guided OMI insertion and have considered deviations clinically acceptable, to date we are missing a defined maximum tolerance level for deviations in one-visit protocols. As the popularity of mini-implant applications in orthodontics is ongoing and due to the high potential of guided insertion, further studies on this topic are indispensable. Additional research is absolutely essential to explore the required accuracy for the simultaneous insertion of mini-implants and TAD-based appliances and to define clear tolerance limits for individually fabricated appliance insertion. Further studies should validate Ludwig et al.'s (53) findings that sterilized insertion guides deliver higher transfer accuracy and should also investigate the use of surgical guides with and without pilot drilling. In dental implantology, milled surgical guides are already deemed superior in accuracy compared with 3D printed templates (145). Schwaerzler et al. (94) were the first to recently compare the transfer accuracy of 3D printed and CAD/CAM milled surgical guides on typodonts, discovering similar deviations between both methods. The mean coronal deviations in the printed group ranged from 0.15 ± 0.20 mm to 0.71 ± 0.22 mm, while in the milled group they were observed to range from 0.09 ± 0.15 mm to 0.83 ± 0.23 mm (94). Further studies examining milled surgical templates are necessary to determine whether this method can offer superior accuracy, as it does in dental implantology, and whether this fabrication process can be adopted in orthodontics. Another underexplored yet interesting option made possible by CBCT based guided implantation is bicortical insertion, with implants showing improved stability, better mechanical outcomes and reduced deformation and fracture (136).

Conclusion

Guided mini-implant insertion is a precise and reliable method nowadays widely used in clinical practice, although slight deviations in transfer accuracy have been shown. The ability to implement a one-visit protocol represents a significant benefit of digitally planned surgical guides compared to freehand insertion. The application of a complete digital workflow streamlines the appliance fabrication and OMI insertion process, consequently reducing the number of required appointments.

Our study revealed that mini-implant insertion was more reliable using commercially available insertion guides compared with in-house self-fabricated surgical templates. Hence outsourcing the planning and fabrication of CAD/CAM surgical guides may be advantageous for certain indications.

Further studies defining tolerance thresholds for positional deviations are necessary. The continuing advancements in digital technologies point to a promising future for guided mini-implant insertion and corresponding appliances.

Bibliography

(1) Proffit, W.; Fields, H.; Larson, B.; Sarver, D. Contemporary orthodontics. Sixth edition ed. Philadelphia, PA: Elsevier; **2019**.

(2) Baumgaertel, S.; Razavi, M.R.; Hans, M.G. Mini-implant anchorage for the orthodontic practitioner. Am. J. Orthod. Dentofac. Orthop. **2008**, 133, 621-627.

(3) Schätzle, M.; Männchen, R.; Zwahlen, M.; Lang, N.P. Survival and failure rates of orthodontic temporary anchorage devices: a systematic review. Clin. Oral. Impl. Res. **2009**, 20, 1351-1359.

(4) Sander, F.; Schwenzer, N.; Ehrenfeld, M. Zahn-Mund-Kieferheilkunde: Kieferorthopädie. 2. Auflage Stuttgart: Thieme Verlagsgruppe; **2011**.

(5) Angle, E.H. Treatment of malocclusion of the teeth: Angle's system. White dental manufacturing Company; **1907**.

(6) Diedrich, P. Different orthodontic anchorage systems. A critical examination. Fortschr. Kieferorthop. **1993**, 54,156-171.

(7) Al-Awadhi, E.A.; Garvey, T.M.; Alhag, M.; Claffey, N.M.; O'Connell, B. Efficacy of the Nance appliance as an anchorage-reinforcement method. Am. J. Orthod. Dentofac. Orthop. **2015**, 147, 330-338.

(8) Diar-Bakirly, S.; Feres, M.F.N.; Saltaji, H.; Flores-Mir, C.; El-Bialy, T. Effectiveness of the transpalatal arch in controlling orthodontic anchorage in maxillary premolar extraction cases: A systematic review and meta-analysis. Angle Orthod. **2017**, 87, 147-158.

(9) Nance, H.N. The limitations of orthodontic treatment: I. Mixed dentition diagnosis and treatment. Am. J. Orthod. Oral Surg. **1947**, 33, 177-223.

(10) Kloehn, S.J. Guiding alveolar growth and eruption of teeth to reduce treatment time and produce a more balanced denture and face. Angle Orthod. **1947**, 17, 10-33.

(11) Jambi, S.; Thiruvenkatachari, B.; D O'Brien, K.; Walsh, T. Orthodontic treatment for distalising upper first molars in children and adolescents. Cochrane Database of Systematic Reviews **2013**.

(12) Kloehn, S.J. Orthodontics--force or persuasion. Angle Orthod. **1953**, 23, 56-65.

(13) Cole, W.A. Accuracy of patient reporting as an indication of headgear compliance. Am. J. Orthod. Dentof. Orthop. **2002**, 121, 419-423.

(14) Wehrbein, H.; Merz, B.R.; Diedrich, P.; Glatzmaier, J. The use of palatal implants for orthodontic anchorage. Design and clinical application of the orthosystem. Clin. Oral Impl. Res. **1996**, 7, 410-416.

(15) Gainsforth, B.L.; Higley, L.B. A study of orthodontic anchorage possibilities in basal bone. Am. J. Orthod. Oral Surg. **1945**, 31, 406-417.

(16) Linkow, L.I. The endosseous blade implant and its use in orthodontics. Int. J. Orthod. **1969**, 7, 149-154.

(17) Brånemark, P.; Breine, U.; Adell, R.; Hansson, B.O.; Lindström, J.; Ohlsson, Å. Intra-osseous anchorage of dental prostheses: I. Experimental studies. Scand. J. Plast. Reconstr. Surg. **1969**, 3, 81-100.

(18) Sherman, A.J. Bone reaction to orthodontic forces on vitreous carbon dental implants. Am. J. Orthod. **1978**, 74, 79-87.

(19) Turley, P.K.; Shapiro, P.A.; Moffett, B.C. The loading of bioglass-coated aluminium oxide implants to produce sutural expansion of the maxillary complex in the pigtail monkey (Macaca nemestrina). Arch. Oral Biol. **1980**, 25, 459-469.

(20) Adell, R.; Lekholm, U.; Rockler, B.; Brånemark, P.I. A 15-year study of osseointegrated implants in the treatment of the edentulous jaw. Int. J. Oral Surg. **1981**, 10, 387-416.

(21) Creekmore, T.D. The possibility of skeletal anchorage. J. Clin. Orthod. **1983**, 17, 266-269.

(22) Roberts, W.E.; Smith, R.K.; Zilberman, Y.; Mozsary, P.G.; Smith, R.S. Osseous adaptation to continuous loading of rigid endosseous implants. Am. J. Orthod. **1984**, 86, 95-111.

(23) Turley, P.K.; Kean, C.; Schur, J.; Stefanac, J.; Gray, J.; Hennes, J. Orthodontic force application to titanium endosseous implants. Angle Orthod. **1988**, 58, 151-162.

(24) Roberts, W.E.; Marshall, K.J.; Mozsary, P.G. Rigid endosseous implant utilized as anchorage to protract molars and close an atrophic extraction site. Angle Orthod. **1990**, 60, 135-152.

(25) Triaca, A.; Antonini, M.; Wintermantel, E. Ein neues titan-Flachschrauben-Implantat zur orthodontischen Verankerung am anterioren Gaumen. Inf. Orthod. Kieferorthop. **1992**, 24, 251-257.

(26) Higuchi, K.W.; Slack, J.M. The use of titanium fixtures for intraoral anchorage to facilitate orthodontic tooth movement. Int. J. Oral. Maxillofac. Impl. **1991**, 6.

(27) Glatzmaier, J.; Wehrbein, H.; Diedrich, P. The development of a resorbable implant system for orthodontic anchorage. The BIOS implant system. Bioresorbable implant anchor for orthodontic systems. Fortschr. Kieferorthop. **1995,** 56, 175-181.

(28) Block, M.S.; Hoffman, D.R. A new device for absolute anchorage for orthodontics. Am. J. Orthod. Dentofac. Orthop. **1995**, 107, 251-258.

(29) Kanomi, R. Mini-implant for orthodontic anchorage. J. Clin. Orthod. **1997**, 31, 763-767.

(30) Park, H.S. The skeletal cortical anchorage using titanium microscrew implants. Korea J. Ort-Od. **1999**, 29, 699 -706.

(31) Umemori, M.; Sugawara, J.; Mitani, H.; Nagasaka, H.; Kawamura, H. Skeletal anchorage system for open-bite correction. Am. J. Orthod. Dentofac. Orthop. **1999**, 115, 166-174.

(32) Jambi, S.; Walsh, T.; Sandler, J.; Benson, P.E.; Skeggs, R.M.; D O'Brien, K. Reinforcement of anchorage during orthodontic brace treatment with implants or other surgical methods. Cochrane Database of Systematic Reviews. **2014**.

(33) Prabhu, J.; Cousley, R.R. Current products and practice: bone anchorage devices in orthodontics. J.Orthod. **2006**, 33, 288-307.

(34) Cope, J.B. Temporary anchorage devices in orthodontics: a paradigm shift. Seminars in orthodontics. WB Saunders. **2005**, 11, 3-9.

(35) Ludwig, B. Mini-Implantate in der Kieferorthopädie: innovative Verankerungskonzepte. Quintessenz-Verlag-GmbH; **2007**.

(36) Ichinohe, M.; Motoyoshi, M.; Inaba, M.; Uchida, Y.; Kaneko, M.; Matsuike, R. Risk factors for failure of orthodontic mini-screws placed in the median palate. J.Oral Sci. **2019**, 61, 13-18.

(37) Cornelis, M.A.; Scheffler, N.R.; De Clerck, H.J.; Tulloch, J.C.; Behets, C.N. Systematic review of the experimental use of temporary skeletal anchorage devices in orthodontics. Am. J. Orthod. Dentofac. Orthop. **2007**, 131, 52-58.

(38) Baumgaertel, S. Cortical bone thickness and bone depth of the posterior palatal alveolar process for mini-implant insertion in adults. Am. J. Orthod. Dentofac. Orthop. **2011**, 140, 806-811.

(39) Scholz, R.P.; Baumgaertel, S. State of the art of miniscrew implants: An interview with Sebastian Baumgaertel**.** Am. J. Orthod. Dentofac. Orthop. **2009**, 136, 277-281.

(40) Holberg, C.; Winterhalder, P.; Holberg, N.; Rudzki-Janson, I.; Wichelhaus, A. Direct versus indirect loading of orthodontic miniscrew implants—an FEM analysis. Clin.Oral Investig. **2013**, 17, 1821-1827.

(41) Baumgaertel, S. Hard and soft tissue considerations at mini-implant insertion sites. J.Orthod. **2014**, 41.

(42) Ludwig, B.; Glasl, B.; Bowman, S.J.; Wilmes, B.; Kinzinger, G.S.; Lisson, J.A. Anatomical guidelines for miniscrew insertion: palatal sites. J.Clin.Orthod. **2011**, 45, 433-41.

(43) Wehrbein, H.; Glatzmaier, J.; Mundwiller, U.; Diedrich, P. The Orthosystem—a new implant system for orthodontic anchorage in the palate. J. Orofac. Orthop. Fortschritte der Kieferorthopädie. **1996**, 57, 142-153.

(44) Wilmes, B.; Ludwig, B.; Vasudavan, S.; Nienkemper, M.; Drescher, D. The T-Zone: Median vs. Paramedian Insertion of Palatal Mini-Implants. J.Clin.Orthod. **2016**, 50, 543-551.

(45) Bernhart, T.; Vollgruber, A.; Gahleitner, A.; Dörtbudak, O.; Haas, R. Alternative to the median region of the palate for placement of an orthodontic implant. Clin.Oral Impl. Res. **2000**, 11, 595-601.

(46) Baumgaertel, S. Quantitative investigation of palatal bone depth and cortical bone thickness for mini-implant placement in adults. Am. J. Orthod. Dentofac. Orthop. **2009**, 136, 104-108.

(47) Hourfar, J.; Ludwig, B.; Bister, D.; Braun, A.; Kanavakis, G. The most distal palatal ruga for placement of orthodontic mini-implants. Eur. J. Orthod. **2015**, 37, 373-378.

(48) Kim, H.; Moon, S.; Lee, S.; Park, Y. Three-dimensional biometric study of palatine rugae in children with a mixed-model analysis: a 9-year longitudinal study. Am. J. Orthod. Dentofac. Orthop. **2012**, 141, 590-597.

(49) Becker, K.; Unland, J.; Wilmes, B.; Tarraf, N.E.; Drescher, D. Is there an ideal insertion angle and position for orthodontic mini-implants in the anterior palate? A CBCT study in humans. Am. J. Orthod. Dentofac. Orthop. **2019,** 156, 345-354.

(50) Asscherickx, K.; Hanssens, J.; Wehrbein, H.; Sabzevar, M.M. Orthodontic anchorage implants inserted in the median palatal suture and normal transverse maxillary growth in growing dogs: a biometric and radiographic study. Angle Orthod. **2005**, 75, 826-831.

(51) Costa, A.; Pasta, G.; Bergamaschi, G. Intraoral hard and soft tissue depths for temporary anchorage devices. Seminars in orthodontics, WB Saunders. **2005,** 10-15.

(52) Kim, H.; Yun, H.; Park, H.; Kim, D.; Park, Y. Soft-tissue and cortical-bone thickness at orthodontic implant sites. Am. J. Orthod. Dentofac. Orthop. **2006**, 130, 177-182.

(53) Ludwig, B.; Krause, L.; Venugopal, A. Accuracy of sterile and non-sterile CAD/CAM insertion guides for orthodontic mini-implants. Front. Dent. Med. **2022**.

(54) Tsaousidis, G.; Bauss, O. Einfluss der Insertionsstelle auf die Misserfolgsraten kieferorthopädischer Verankerungsschrauben. J. Orofac. Orthop. Fortschritte der Kieferorthopädie. **2008**, 69, 349-356.

(55) Nienkemper, M.; Ludwig, B. Influence of guided insertion on the success of paramedian palatal miniscrews. Seminars in Orthodontics. WB Saunders. **2023**.

(56) Kuroda, S.; Tanaka, E. Risks and complications of miniscrew anchorage in clinical orthodontics. Jap. Dent. Sci. Rev. **2014**, 50, 79-85.

(57) Mohammed, H.; Wafaie, K.; Rizk, M.Z.; Almuzian, M.; Sosly, R.; Bearn, D.R. Role of anatomical sites and correlated risk factors on the survival of orthodontic miniscrew implants: a systematic review and meta-analysis. Progress in Orthod. **2018**, 19, 1-18.

(58) Arqub, S.A.; Gandhi, V.; Mehta, S.; Palo, L.; Upadhyay, M.; Yadav, S. Survival estimates and risk factors for failure of palatal and buccal mini-implants. Angle Orthod. **2021**, 91, 756-763.

(59) Karagkiolidou, A.; Ludwig, B.; Pazera, P.; Gkantidis, N.; Pandis, N.; Katsaros, C. Survival of palatal miniscrews used for orthodontic appliance anchorage: a retrospective cohort study. Am. J. Orthod. Dentofac. Orthop. **2013**, 143, 767-772.

(60) Gill, G.; Shashidhar, K.; Kuttappa, M.N.; PB, D.K.; Sivamurthy, G.; Mallick, S. Failure rates and factors associated with infrazygomatic crestal orthodontic implants-A prospective study. J. Oral Biolog. Craniofac. Research. **2023**, 13, 283-289.

(61) Chang, C.H.; Lin, J.S.; Roberts, W.E. Failure rates for stainless steel versus titanium alloy infrazygomatic crest bone screws: A single-center, randomized double-blind clinical trial. Angle Orthod. **2019**, 89, 40-46.

(62) Chang, C.; Liu, S.S.; Roberts, W.E. Primary failure rate for 1680 extra-alveolar mandibular buccal shelf mini-screws placed in movable mucosa or attached gingiva. Angle Orthod. **2015**, 85, 905-910.

(63) Sarul, M.; Lis, J.; Park, H.; Rumin, K. Evidence-based selection of orthodontic miniscrews, increasing their success rate in the mandibular buccal shelf. A randomized, prospective clinical trial. BMC Oral Health. **2022**, 22, 414.

(64) Hong, S.; Kusnoto, B.; Kim, E.; BeGole, E.A.; Hwang, H.; Lim, H. Prognostic factors associated with the success rates of posterior orthodontic miniscrew implants: A subgroup meta-analysis. Kor. J. Orthod. **2016**, 46, 111.

(65) Hourfar, J.; Bister, D.; Kanavakis, G.; Lisson, J.A.; Ludwig, B. Influence of interradicular and palatal placement of orthodontic mini-implants on the success (survival) rate. Head & face medicine. **2017**, 13, 1-6.

(66) Baumgaertel, S. Maxillary molar movement with a new treatment auxiliary and palatal miniscrew anchorage. J.Clin.Orthod. **2008**, 42, 587-589.

(67) Baumgaertel, S. Hard and soft tissue considerations at mini-implant insertion sites. J.Orthod. **2014**, 41, 3-7.

(68) Kuroda, S.; Yamada, K.; Deguchi, T.; Hashimoto, T.; Kyung, H.; Yamamoto, T.T. Root proximity is a major factor for screw failure in orthodontic anchorage. Am. J. Orthod. Dentofac. Orthop. **2007**, 131, 68-73.

(69) Asscherickx, K.; Vannet, B.V.; Wehrbein, H.; Sabzevar, M.M. Success rate of miniscrews relative to their position to adjacent roots. Europ. J. Orthod. **2008**, 30, 330-335.

(70) Kim, H.; Kim, T. Histologic evaluation of root-surface healing after root contact or approximation during placement of mini-implants. Am. J. Orthod. Dentofac. Orthop. **2011**, 139, 752-760.

(71) Asscherickx, K.; Vannet, B.V.; Wehrbein, H.; Sabzevar, M.M. Root repair after injury from mini-screw. Clin.Oral Implants Res. **2005**, 16, 575-578.

(72) Kadioglu, O.; Büyükyilmaz, T.; Zachrisson, B.U.; Maino, B.G. Contact damage to root surfaces of premolars touching miniscrews during orthodontic treatment. Am. J. Orthod. Dentofac. Orthop. **2008**, 134, 353-360.

(73) Lee, J.Y.; Kim, P.S.; Choi, C.; Kim, K.B. Root repair and regeneration after miniscrew root damage. J. World Fed. Orthod. **2016**, 5, 70-78.

(74) Liou, E.J.; Pai, B.C.; Lin, J.C. Do miniscrews remain stationary under orthodontic forces? Am. J. Orthod. Dentofac. Orthop. **2004**, 126, 42-47.

(75) Poggio, P.M.; Incorvati, C.; Velo, S.; Carano, A. “Safe zones”: a guide for miniscrew positioning in the maxillary and mandibular arch. Angle Orthod. **2006**, 76, 191-197.

(76) Kravitz, N.D.; Kusnoto, B. Risks and complications of orthodontic miniscrews. Am. J. Orthod. Dentofac. Orthop. **2007**, 131, 43-51.

(77) Brånemark, P.I.; Adell, R.; Albrektsson, T.; Lekholm, U.; Lindström, J.; Rockler, B. An experimental and clinical study of osseointegrated implants penetrating the nasal cavity and maxillary sinus. J. Oral Maxillofac. Surgery. **1984**, 42, 497-505.

(78) Ardekian, L.; Oved-Peleg, E.; Mactei, E.E.; Peled, M. The clinical significance of sinus membrane perforation during augmentation of the maxillary sinus. J. Oral Maxillofac. Surgery **2006**, 64, 277-282.

(79) Motoyoshi, M.; Sanuki-Suzuki, R.; Uchida, Y.; Saiki, A.; Shimizu, N. Maxillary sinus perforation by orthodontic anchor screws. J.Oral Sci. **2015**, 57, 95-100.

(80) Moghadam, H.G.; Caminiti, M.F. Life-threatening hemorrhage after extraction of third molars: case report and management protocol. J. Canad. Dent. Assoc. **2002**, 68, 670-675.

(81) Fäh, R.; Schätzle, M. Complications and adverse patient reactions associated with the surgical insertion and removal of palatal implants: a retrospective study. Clin.Oral Implants Res. **2014**, 25, 653-658.

(82) Ozen, T.; Orhan, K.; Gorur, I.; Ozturk, A. Efficacy of low level laser therapy on neurosensory recovery after injury to the inferior alveolar nerve. Head & face medicine. **2006**, 2, 1-9.

(83) Federick, D.R.; Del Rey, M. A surgical guide for insertion of implant fixtures. Implant Dent. **1992**, 1, 129-133.

(84) Möhlhenrich, S.C.; Brandt, M.; Kniha, K.; Prescher, A.; Holzle, F.; Modabber, A. Accuracy of orthodontic mini-implants placed at the anterior palate by tooth-borne or gingiva-borne guide support: a cadaveric study. Clin.Oral Investig. **2019**, 23, 4425-4431.

(85) Nienkemper, M.; Ludwig, B. Risk of root damage after using lateral cephalogram and intraoral scan for guided insertion of palatal miniscrews. Head & face medicine. **2022**, 18, 30.

(86) Cousley, R.R. A stent-guided mini-implant system. J. Clin. Orthod. **2009**, 43, 403-407.

(87) Maino, B.G.; Paoletto, E.; Lombardo, L.; Siciliani, G. A Three-Dimensional Digital Insertion Guide for Palatal Miniscrew Placement. J.Clin.Orthod. **2016**, 50, 12-22.

(88) Suzuki, E.Y.; Suzuki, B. Accuracy of miniscrew implant placement with a 3-dimensional surgical guide. J. Oral Maxillofac. Surg. **2008**, 66, 1245-1252.

(89) Martin, W.; Heffernan, M.; Ruskin, J. Template fabrication for a midpalatal orthodontic implant. Int. J. Oral Maxillofac. Implants. **2002**, 17.

(90) Tosun, T.; Keles, A.; Erverdi, N. Method for the placement of palatal implants. Int. J. Oral Maxillofac. Implants **2002**, 17.

(91) Cassetta, M.; Altieri, F.; Di Giorgio, R.; Barbato, E. Palatal orthodontic miniscrew insertion using a CAD-CAM surgical guide: description of a technique. Int. J. Oral Maxillofac. Surg. **2018**, 47, 1195-1198.

(92) Bae, M.J.; Kim, J.Y.; Park, J.T.; Cha, J.Y.; Kim, H.J.; Yu, H.S. Accuracy of miniscrew surgical guides assessed from cone-beam computed tomography and digital models. Am. J. Orthod. Dentofac. Orthop. **2013**, 143, 893-901.

(93) Liu, H.; Liu, D.X.; Wang, G.; Wang, C.L.; Zhao, Z. Accuracy of surgical positioning of orthodontic miniscrews with a computer-aided design and manufacturing template. Am. J. Orthod. Dentofac. Orthop. **2010**, 137, 728, 1-9.

(94) Schwärzler, A.; Ludwig, B.; Chitan, P.; Lettner, S.; Sagl, B.; Jonke, E. Transfer accuracy of 3D printed versus CAD/CAM milled surgical guides for temporary orthodontic implants: A preclinical micro CT study. J. Dent. **2024**, 146, 105060.

(95) Migliorati, M.; Drago, S.; Pozzan, L.; Contardo, L. Does the planned miniscrew position reflect the achieved one? A clinical study on the reliability of guided miniscrew insertion using lateral cephalogram and maxillary stereolithography file for planning. Am. J. Orthod. Dentofac. Orthop. **2022**, 162, 312-318.

(96) Kirnbauer, B.; Rugani, P.; Santigli, E.; Tepesch, P.; Ali, K.; Jakse, N. Fully guided placement of orthodontic miniscrews-a technical report. Australas. Orthod. J. **2019**, 35, 71-74.

(97) Vasoglou, G.; Stefanidaki, I.; Apostolopoulos, K.; Fotakidou, E.; Vasoglou, M. Accuracy of Mini-Implant Placement Using a Computer-Aided Designed Surgical Guide, with Information of Intraoral Scan and the Use of a Cone-Beam CT. Dent. J. **2022**, 8,10,104.

(98) Mang de la Rosa, M.R.; Safaltin, A.; Jost-Brinkmann, P.; Aigner, A.; Koch P.J. Accuracy of palatal orthodontic mini-implants placed by conventionally or CAD/CAM-based surgical guides: a comparative in vitro study. Angle Orthod. **2023**, 93, 79-87.

(99) Yu, J.H.; Wang, Y.T.; Lin, C.L. Customized surgical template fabrication under biomechanical consideration by integrating CBCT image, CAD system and finite element analysis. Dent. Mater. J. **2018**, 30, 37, 6-14.

(100) Willmann, J.; Wilmes, B.; Becker, K.; Drescher, D. Hybrid Hyrax Direct Eine neue Technik zur maxillären Expansion und Protraktion. Kieferorthopädie. **2020**.

(101) Küffer, M.; Drescher, D.; Becker, K. Application of the Digital Workflow in Orofacial Orthopedics and Orthodontics: Printed Appliances with Skeletal Anchorage. Appl. Sci. **2022**, 12, 3820.

(102) Kühl, S.; Payer, M.; Zitzmann, N.U.; Lambrecht, J.T.; Filippi, A. Technical Accuracy of Printed Surgical Templates for Guided Implant Surgery with the coDiagnostiX TM Software. Clin. Implant Dent. Relat. Res. **2015**, 17, 177-182.

(103) Jung, R.E.; Schneider, D.; Ganeles, J.; Wismeijer, D.; Zwahlen, M.; Hammerle, C. Computer technology applications in surgical implant dentistry: a systematic review. DARE: Quality-assessed Reviews [Internet]. **2009**.

(104) Tarraf, N. E.; Ali, D. M. Present and the future of digital orthodontics. Seminars in Orthodontics. WB Saunders. **2018**, 376-385.

(105) Panayi, N.C.; Efstathiou, S.; Christopoulou, I.; Kotantoula, G.; Tsolakis, I.A. Digital orthodontics: Present and future. Am. J. Orthod. Dentofac. Orthop. **2024**, 4, 14-25.

(106) Vandenberghe, B. The digital patient–Imaging science in dentistry. J. Dent. **2018**, 74, 21-26.

(107) Federici Canova, F.; Oliva, G.; Beretta, M.; Dalessandri, D. Digital (R) Evolution: Open-source softwares for orthodontics. Appl. Sci. **2021**, 11, 6033.

(108) Wang, C.H.; Randazzo, L. Evolution of imaging and management systems in orthodontics. Am. J. Orthod. Dentofac. Orthop. **2016**, 149, 798-805.

(109) Marradi, F.; Staderini, E.; Zimbalatti, M.A.; Rossi, A.; Grippaudo, C.; Gallenzi, P. How to obtain an orthodontic virtual patient through superimposition of three-dimensional data: A systematic review. Appl. Sci. **2020**, 10, 5354.

(110) Willmann, J.H.; Wilmes, B.; Chhatwani, S.; Drescher, D. Klinische Anwendung des digitalen Workflows am Beispiel von Mini-Implantaten. Informationen Orthod. Kieferorthopädie. **2020**, 52, 121-127.

(111) Choi, Y.; Kim, M.; Lee, J.; Kang, S. Impact of the number of registration points for replacement of three-dimensional computed tomography images in dental areas using three-dimensional light-scanned images of dental models. Oral Rad. **2014**, 30, 32-37.

(112) Vandenberghe, B. The crucial role of imaging in digital dentistry. Dent. Mat. **2020**, 36, 581-591.

(113) Kim, Y.; Lim, S.; Gang, S. Comparison of cephalometric measurements and cone-beam computed tomography-based measurements of palatal bone thickness. Am. J. Orthod. Dentofac. Orthop. **2014**, 145, 165-172.

(114) Eigenwillig, P.; Chhatwani, S.; Ludwig, B. Digitaler Workflow bei der Anwendung von Miniimplantaten. Kieferorthopädie. **2017**, 31, 411-416.

(115) Sehrawat, S.; Kumar, A.; Prabhakar, M.; Nindra, J. The expanding domains of 3D printing pertaining to the speciality of orthodontics. Mat. today: Proceedings. **2022,** 50, 1611-1618.

(116) Graf, S.; Thakkar, D.; Hansa, I.; Pandian, S. M.; & Adel, S. M. 3D Metal Printing in Orthodontics: Current Trends, Biomaterials, Workflows and Clinical Implications. Seminars in Orthodontics. WB Saunders. **2023**, 34-42.

(117) Tian, Y.; Chen, C.; Xu, X.; Wang, J.; Hou, X.; Li, K. A review of 3D printing in dentistry: Technologies, affecting factors, and applications. Scanning. **2021**.

(118) Graf, S.; Cornelis, M.A.; Gameiro, G.H.; Cattaneo, P.M. Computer-aided design and manufacture of hyrax devices: can we really go digital? Am. J. Orthod. Dentofac. Orthop. **2017**, 152, 870-874.

(119) Thiel, W. Supplement to the conservation of an entire cadaver according to W. Thiel. Ann. Anat. **2002**, 184, 267–269.

(120) Kniha, K.; Brandt, M.; Bock, A.; Modabber, A.; Prescher, A.; Hölzle, F. Accuracy of fully guided orthodontic mini-implant placement evaluated by cone-beam computed tomography: a study involving human cadaver heads. Clin.Oral Investig. **2020**.

(121) Suzuki, E.Y.; Suzuki, B.Accuracy of miniscrew implant placement with a 3-dimensional surgical guide. J.Oral Maxillofac. Surg. **2008**, 66, 1245-1252.

(122) Miyazawa, K.; Kawaguchi, M.; Tabuchi, M.; Goto, S. Accurate pre-surgical determination for self-drilling miniscrew implant placement using surgical guides and cone-beam computed tomography. Europ. J. Orthod. **2010**, 32, 735-740.

(123) Su, L.; Song, H.; Huang, X. Accuracy of two orthodontic mini-implant templates in the infrazygomatic crest zone: a prospective cohort study. BMC Oral Health. **2022,** 24, 22, 252-0.

(124) Jedliński, M.; Janiszewska-Olszowska, J.; Mazur, M.; Ottolenghi, L.; Grocholewicz, K.; Galluccio, G. Guided Insertion of Temporary Anchorage Device in Form of Orthodontic Titanium Miniscrews with Customized 3D Templates—A Systematic Review with Meta-Analysis of Clinical Studies. Coatings. **2021**, 11, 1488.

(125) Baumgaertel, S.; Palomo, J.M.; Palomo, L.; Hans, M.G. Reliability and accuracy of cone-beam computed tomography dental measurements. Am. J. Orthod. Dentofac. Orthop. **2009**, 136, 19-25.

(126) Migliorati, M.; De Mari, A.; Annarumma, F.; Aghazada, H.; Battista, G.; Campobasso, A. Three-dimensional analysis of miniscrew position changes during bone-borne expansion in young and late adolescent patients. Prog Orth. **2023**, 24, 1–13.

(127) Iodice, G.; Nanda, R.; Drago, S.; Repetto, L.; Tonoli, G.; Silvestrini-Biavati, A. Accuracy of direct insertion of TADs in the anterior palate with respect to a 3D-assisted digital insertion virtual planning. Orthod. Craniofac. Res. **2021**.

(128) Costalos, P.A.; Sarraf, K.; Cangialosi, T.J.; Efstratiadis, S. Evaluation of the accuracy of digital model analysis for the American Board of Orthodontics objective grading system for dental casts. Am. J. Orthod. Dentofac. Orthop. **2005**, 128, 624-629.

(129) Qiu, L.; Haruyama, N.; Suzuki, S.; Yamada, D.; Obayashi, N.; Kurabayashi, T. Accuracy of orthodontic miniscrew implantation guided by stereolithographic surgical stent based on cone-beam CT-derived 3D images. Angle Orthod. **2012**, 82, 284-293.

(130) Lin, H.; Chiang, W.; Lo, L.; Hsu, S.S.; Wang, C.; Wan, S. Artifact-resistant superimposition of digital dental models and cone-beam computed tomography images. J. Oral Maxillofac. Surg. **2013**, 71, 1933-1947.

(131) Dot, G.; Rafflenbeul, F.; Salmon, B. Voxel-based superimposition of Cone Beam CT scans for orthodontic and craniofacial follow-up: Overview and clinical implementation. Internat. Orthod. **2020**, 18, 739-748.

(132) Jung, B.A.; Wehrbein, H.; Heuser, L.; Kunkel, M. Vertical palatal bone dimensions on lateral cephalometry and cone-beam computed tomography: implications for palatal implant placement. Clin. Oral Implants Res. **2011**, 22, 664-668.

(133) von See, C.; Wagner, M.E.; Schumann, P.; Lindhorst, D.; Gellrich, N.; Stoetzer, M. Non-radiological method for three-dimensional implant position evaluation using an intraoral scan method. Clin. Oral Implants Res. **2014**, 25, 1091-1093.

(134) Stoetzer, M.; Wagner, M.E.; Wenzel, D.; Lindhorst, D.; Gellrich, N.; von See, C. Nonradiological method for 3-dimensional implant position assessment using an intraoral scan: new method for postoperative implant control. Implant Dent. **2014**, 23, 612-616.

(135) Wilhelmy, L.; Willmann, J.H.; Tarraf, N.E.; Wilmes, B.; Drescher, D. Maxillary space closure using a digital manufactured Mesialslider in a single appointment workflow. Korean J. Orthod. **2022**, 52, 236-245.

(136) Pozzan, L.; Migliorati, M.; Dinelli, L.; Riatti, R.; Torelli, L.; Di Lenarda, R. Accuracy of the digital workflow for guided insertion of orthodontic palatal TADs: a step-by-step 3D analysis. Prog. Orthod. **2022**, 23, 27-6.

(137) Perinetti, G.; Tonini, P.; Bruno, A. Inserzione guidata di miniviti ortodontiche: il sistema di pianificazione 'REPLICA.'. **2020**, 5, 23-33.

(138) Tahmaseb, A.; Wu, V.; Wismeijer, D.; Coucke, W.; Evans, C. The accuracy of static computer-aided implant surgery: A systematic review and meta-analysis. Clin. Oral Implants Res. **2018**, 29, 416-435.

(139) Wilmes, B.; Nanda, R.; Nienkemper, M.; Ludwig, B.; Drescher, D. Correction of upper-arch asymmetries using the Mesial-Distalslider. J. Clin. Orthod. **2013**, 47, 648-655.

(140) Hourfar, J.; Kanavakis, G.; Bister, D.; Schätzle, M.; Awad, L.; Nienkemper, M. Three dimensional anatomical exploration of the anterior hard palate at the level of the third ruga for the placement of mini-implants--a cone-beam CT study. Eur. J. Orthod. **2015**, 37, 589-595.

(141) Ashton, K.Y.; Jiang, S.S.; Melo, M.A.; Bosio, J.A. International investigation on temporary anchorage device use: A survey of orthodontists. J. World Fed. Orthod. **2023**, 12, 93-104.

(142) Budsabong, C.; Trachoo, V.; Pittayapat, P.; Chantarawaratit, P. The association between thread pitch and cortical bone thickness influences the primary stability of orthodontic miniscrew implants: a study in human cadaver palates. J. World Fed. Orthod. **2022**, 11, 68-73.

(143) Chhatwani, S.; Rose-Zierau, V.; Haddad, B.; Almuzian, M.; Kirschneck, C.; Danesh, G. Three-dimensional quantitative assessment of palatal bone height for insertion of orthodontic implants-a retrospective CBCT study. Head & face medicine. **2019**, 15, 1-8.

(144) Bourassa, C.; Hosein, Y.K.; Pollmann, S.I.; Galil, K.; Bohay, R.N.; Holdsworth, D.W. In-vitro comparison of different palatal sites for orthodontic miniscrew insertion: Effect of bone quality and quantity on primary stability. Am. J. Orthod. Dentofac. Orthop. **2018** ,154, 809-819.

(145) Park, J.; Yi, T.; Koak, J.; Kim, S.; Park, E.; Heo, S. Comparison of five-axis milling and rapid prototyping for implant surgical templates. Int. J. Oral Maxillofac. Implants **2014**, 29.

The following tool was used to optimize the language of the text:

- ChatGPT, Version: GPT-3.5 (free version)
- OpenAI (San Francisco, California, USA)
- 19.10.2023 – 07.10.2024
- https://chat.openai.com/